

Quantifying nonclassicality of vacuum-one-photon superpositions via potentials for Bell nonlocality, quantum steering, and entanglement

Adam Miranowicz,^{1,2} Josef Kadlec,³ Karol Bartkiewicz,¹ Antonín Černoč,⁴ Yueh-Nan Chen,^{5,6} Karel Lemr,³ and Franco Nori^{2,7,8}

¹*Institute of Spintronics and Quantum Information, Faculty of Physics, Adam Mickiewicz University, 61-614 Poznań, Poland*

²*Theoretical Quantum Physics Laboratory, Cluster for Pioneering Research, RIKEN, Wakoshi, Saitama 351-0198, Japan*

³*Joint Laboratory of Optics of Palacký University and Institute of Physics of Czech Academy of Sciences, 17. listopadu 12, 779 00 Olomouc, Czech Republic*

⁴*Institute of Physics of the Czech Academy of Sciences, Joint Laboratory of Optics of PU and IP AS CR, 17. listopadu 50A, 772 07 Olomouc, Czech Republic*

⁵*Department of Physics, National Cheng Kung University, Tainan 70101, Taiwan*

⁶*Center for Quantum Frontiers of Research & Technology, NCKU, Tainan 70101, Taiwan*

⁷*Center for Quantum Computing, RIKEN, Wakoshi, Saitama 351-0198, Japan*

⁸*Department of Physics, University of Michigan, Ann Arbor, Michigan 48109-1040, USA*

(Dated: September 25, 2023)

Entanglement potentials are popular measures of the nonclassicality of single-mode optical fields. These potentials are defined by the amount of entanglement (measured by, e.g., the negativity or concurrence) of the two-mode field generated by mixing a given single-mode field with the vacuum on a balanced beam splitter. We generalize this concept to define the potentials for Bell nonlocality and quantum steering in specific measurement scenarios, in order to quantify single-mode nonclassicality in a more refined way. Thus, we can study the hierarchy of three types of potentials in close analogy to the well-known hierarchy of the corresponding two-mode quantum correlations. For clarity of our presentation, we focus on the analysis of the nonclassicality potentials for arbitrary vacuum-one-photon superpositions (VOPSs), corresponding to a photon-number qubit. We discuss experimentally feasible implementations for the generation of single-mode VOPS states, their mixing with the vacuum on a balanced beam splitter, and their two-mode Wigner-function reconstruction using homodyne tomography to determine the potentials. We analyze the effects of imperfections, including phase damping and unbalanced beam splitting on the quality of the reconstructed two-mode states and nonclassicality potentials. Although we focus on the analysis of VOPS states, single-mode potentials can also be applied to study the nonclassicality of qudits or continuous-variable systems.

I. INTRODUCTION

Nonclassical optical states (including entangled, squeezed, or photon antibunched) are the main resources for quantum technologies and quantum information processing with photons. Thus, testing and quantifying the nonclassicality (NC) of optical states has been attracting attention in quantum physics since the pioneering work of Kennard [1] on squeezed states published almost a century ago. It is worth noting that the first truly convincing experimental demonstration of the nonclassical character of photons was based on measuring photon antibunching [2]. Recent experimental optical demonstrations of quantum advantage include enhanced gravitational-wave detection with squeezed states [3–5], boson sampling based on entangled and squeezed states [6–8], and entanglement-based quantum cryptography [9].

In quantum optics, the state of an optical field is classified as nonclassical (or quantum) if its Glauber-Sudarshan P function [10, 11] is not positive semidefinite, so it is not a classical probability density [12–14]. This means that only coherent states and their statistical mixtures are considered classical. Extensive attention has been devoted to various forms of nonclassical

cal correlations, with particular emphasis on their three distinct types: quantum entanglement (quantum inseparability) [15], Einstein-Podolsky-Rosen (EPR) steering (commonly referred to as quantum steering) [16, 17], and Bell nonlocality, which manifests through violations of Bell inequalities [18]. In this paper, we quantify the NC of single-qubit optical states, which are arbitrary vacuum and one-photon superpositions (VOPS), via measures of two-mode quantum correlations. Testing nonlocal quantum correlations of single-photon states, or more specifically the states, generated by mixing a VOPS with the vacuum on a balanced beam splitter (BS), has been attracting considerable interest both theoretical (see, e.g., [19–22]) and experimental (see, e.g., [23–26]).

Experimental tests whether a given optical state is nonclassical are usually based on measuring NC witnesses corresponding to demonstrating violations of various classical inequalities [14, 27–30]. Typical NC witnesses are not universal, which means that they are sufficient but not necessary criteria of NC. Universal witnesses of NC correspond to those criteria which are both sufficient and necessary of NC. Experimental implementations of such universal witnesses usually require applying a complete quantum state tomography (QST). They

can be used not only as NC tests but also NC measures (if they satisfy some additional properties). The most popular NC measures include: nonclassical distance [31], nonclassical depth [32, 33], and entanglement potentials [34].

Nonclassical depth is defined as the minimal amount of Gaussian noise which transforms a nonpositive semidefinite P function into a positive one. It is equal to 1 for all non-Gaussian states, and, thus, it is not a useful measure to quantify the amount of the NC of VOPS states [35], although it was shown to be useful for quantifying the NC of Gaussian states, e.g., twin beams [36]. Moreover, nonclassical distance is defined as the distance (according to a chosen distance measure including those of Bures or Kullback-Leibler) of a given nonclassical state to its closest classical state (CCS). Finding a CCS is usually very hard, even numerically. Of course, if one limits the set of classical states, then the nonclassical distance can be calculated effectively; e.g., it can be calculated for VOPS states if the vacuum is chosen as the CCS, which is reasonable because this is the only classical VOPS state [35]. Of course, the CCS for a given VOPS state might belong to a wider class of classical states. So, in general, finding a CCS could be difficult even for such simple VOPS states. Thus, we consider here only entanglement potentials and related NC quantifiers which do not suffer from the above-mentioned problems of nonclassical depth and distance.

Non-universal NC witnesses, which are also often used for quantifying NC, to mention only a few include: (i) quadrature squeezing variances; (ii) second-order correlation functions to quantify photon antibunching and the sub-Poissonian photon statistics; (iii) the nonclassical volume corresponding to the volume of the negative part of a Wigner function [37]; (iv) the Wigner distinguishability quantifier [38], which is defined in terms of the distinguishability of a given state from one with a positive Wigner function; and (v) quantifiers of two- and multi-mode quantum correlations, which are the main topic of this paper, can also be used for estimating the degree of NC [34, 35, 39–41]. We also mention operational approaches to quantify the NC of states (see, e.g., [42–44]) including the effect of a measurement setup. For example, the negativity of quantumness is defined as the minimum entanglement (quantified by the negativity) that is created between a given system and a measurement apparatus assuming local measurements performed on subsystems [44].

The well-known hierarchy of standard measures of entanglement, EPR steering (in different measurement scenarios), and Bell nonlocality has recently been demonstrated for experimental polarization-qubit states, which were measured by applying complete [45, 46] or incomplete [47] QST. A closely related hierarchy of temporal quantum correlations, including temporal inseparability, temporal steering, and macrorealism, has also been studied [48]. Moreover, considerable research has been devoted to the hierarchies of measures or witnesses of NC, which are limited to specific types of quantum correla-

tions. These include hierarchies of entanglement witnesses [49, 50], steering witnesses [22], Bell inequalities [18, 51]; as well as spatial [52] and spatiotemporal [29, 53] NC witnesses.

In this paper we study theoretically *the potentials for two-qubit correlations to quantify the NC of single-qubit states defined as (coherent or incoherent) VOPSs*. We focus on analyzing quantifiers of single-qubit NC based on the above-mentioned three types of quantum correlations, i.e., entanglement, steering, and Bell nonlocality. More specifically, inspired by the concept of entanglement potentials introduced in Ref. [34] for quantifying the NC of single-mode optical states, *we introduce the potentials for EPR steering and Bell nonlocality. These potentials for two-mode quantum correlations can serve as the quantifiers of single-mode NC correlations*. In particular, they can also enable us to determine the hierarchy of single-qubit nonclassical correlations via the corresponding hierarchy of two-qubit nonclassical correlations.

Compared to our former related works on quantifying NC of single-qubit optical states [35, 40], here we introduce *novel types of potentials for two-qubit correlations to study the hierarchy of single-qubit nonclassicality*, analogously to the hierarchy of two-qubit correlations, which we studied experimentally in Refs. [45–47] using polarization-based tomographic methods (see Refs. [54, 55] for comparative analyses).

In this work, we use photon-number encoding of qubits, and, thus, we consider Wigner tomographic methods for their reconstruction. For example, a two-mode state (say ρ), which is generated by mixing a VOPS state with the vacuum at a balanced BS, can be reconstructed by homodyne tomography by locally mixing each mode of ρ with a high-intensity classical beam (i.e., a local oscillator), as shown in Fig. 1(a). The reconstructed Wigner functions and, thus, also two-mode density matrices enable the calculation of any quantifiers of two-qubit correlations and the corresponding potentials for single-mode VOPS states. The feasibility of this homodyne-QST-based approach has already been experimentally demonstrated, but only in a special case of the input single-photon Fock state for testing Bell nonlocality [25, 26] and EPR steering [26].

This paper is organized as follows: The concept of entanglement potentials is recalled and the potentials for EPR steering and Bell nonlocality are introduced and analyzed in detail in Sec. II assuming ideal experimental conditions. These concepts are generalized in Sec. III for realistic experimental conditions by including the effects of phase damping and unbalanced beam-splitting (corresponding to amplitude damping). The phase-space approach to describe nonclassicality using the Wigner and generalized Wigner functions (i.e., Cahill-Glauber functions) is given in Sec. IV based on the definitions summarized in Appendix A. Feasible experimental setups for the generation of the VOPS states and the tomographic reconstruction of the corresponding two-qubit states are described in Sec. V A. In Sec. V B we briefly

discuss how nonclassicality potentials can be defined and applied for higher- or even infinite-dimensional systems using NC witnesses rather than NC measures. We conclude in Sec. VI.

II. IDEAL NONCLASSICALITY POTENTIALS

Here, by generalizing the idea of entanglement potentials of Asbóth *et al.* [34], we define other NC potentials, i.e., those related to quantum steering and Bell nonlocality and, then, we use them to classify the NC of single-qubit optical states. We first analyze these potentials under ideal conditions assuming no damping and a perfectly balanced BS.

We consider single-qubit optical states defined as (coherent or incoherent) superpositions of the vacuum $|0\rangle$ and the single-photon Fock state $|1\rangle$, which are (for brevity) referred to as VOPS states, and given by a general density matrix,

$$\sigma(p, x) = \sum_{m,n=0}^1 \sigma_{mn} |m\rangle\langle n| = \begin{bmatrix} 1-p & x \\ x^* & p \end{bmatrix}, \quad (1)$$

where $p \in [0, 1]$ is the probability of measuring a single photon, $p = \langle 1|\sigma|1\rangle$, and x is a coherence parameter satisfying $|x| \in [0, \sqrt{p(1-p)}]$. When referring to the VOPS encoding of qubit states, the only classical state of $\sigma(p, x)$ is for $p = 0$, corresponding to the vacuum.

A. Entanglement potentials for a single qubit

According to the approach of Ref. [34], a NC measure of a single optical qubit σ can be defined by the entanglement of the output state ρ_{out} of an auxiliary lossless balanced beam-splitter (BS) with the state σ and the vacuum $|0\rangle$ at the inputs [see Fig. 1(a)], i.e.,

$$\rho_{\text{out}} = U_{\text{BS}}(\sigma \otimes |0\rangle\langle 0|)U_{\text{BS}}^\dagger, \quad (2)$$

given in terms of the unitary transformation $U_{\text{BS}} = \exp(-iH\theta)$; with the Hamiltonian $H = \frac{1}{2}i(a_1^\dagger a_2 - a_1 a_2^\dagger)$, where $a_{1,2}$ ($a_{1,2}^\dagger$) are the annihilation (creation) operators of the input modes and, for simplicity, we set $\hbar = 1$. Moreover, the BS parameter θ defines the reflection and transmission coefficients, as $r = \sin(\theta/2)$ and $t = \cos(\theta/2)$, respectively.

First, we set $\theta = \pi/2$ for a balanced BS. Linear transformations (as discussed in greater detail in Sec. IV) do not change the global NC of an optical field. Thus, the output state ρ_{out} is entangled if and only if the input state σ is nonclassical. Let us recall that coherent states (so infinite-dimensional states except the vacuum) and their statistical mixtures are the only classical states. Thus, an arbitrary finite-dimensional single-mode optical state (except the vacuum) is nonclassical and if it is mixed with

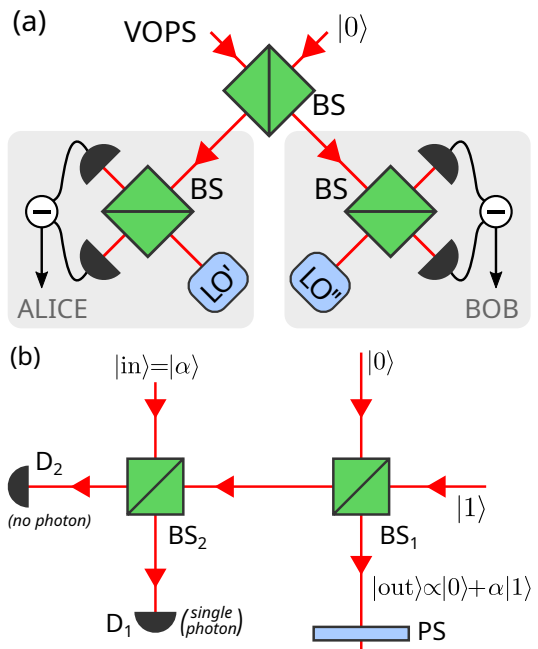


FIG. 1. (a) Scheme for converting the nonclassicality of a vacuum-one-photon superposition (VOPS) state $\sigma(p, x)$ into a two-mode state $\rho(p, x)$ exhibiting entanglement, and in some cases EPR steering and Bell nonlocality; $\rho(p, x)$ can be reconstructed by homodyne state tomography, where LO' and LO'' stand for local oscillators and BS denotes a beam splitter. (b) Quantum scissors device for the nonlocal generation of arbitrary VOPS, where $|\text{in}\rangle = |\alpha\rangle$ is a coherent input state, which is truncated to a qubit state $|\text{out}\rangle$; D_i are single-photon photodetectors, and PS denotes a phase shift (0 or π), which is applied with a specific probability to decohere the state $|\text{out}\rangle$, i.e., to decrease its coherence factor $x = \sqrt{p(1-p)}$ to a desired value.

the vacuum on a BS, then the output two-mode state is entangled.

In a special case, by mixing an arbitrary single-qubit optical state $\sigma(p, x)$ with the vacuum on a perfect balanced BS and assuming no phase and amplitude dissipation, the following state $\rho_{\text{out}} \equiv \rho(p, x)$ is generated:

$$\rho(p, x) = \begin{bmatrix} 1-p & -\frac{1}{\sqrt{2}}x & \frac{1}{\sqrt{2}}x & 0 \\ -\frac{1}{\sqrt{2}}x^* & \frac{1}{2}p & -\frac{1}{2}p & 0 \\ \frac{1}{\sqrt{2}}x^* & -\frac{1}{2}p & \frac{1}{2}p & 0 \\ 0 & 0 & 0 & 0 \end{bmatrix}. \quad (3)$$

To quantify the NC of σ , we consider the entanglement potential [34]:

$$\text{CP}(\sigma) = E(\rho_{\text{out}}), \quad (4)$$

which is defined by, e.g., the Wootters concurrence [56]:

$$C(\rho) = \Theta\left(2 \max_j \lambda_j - \sum_j \lambda_j\right), \quad (5)$$

TABLE I. Four regimes of vanishing or nonvanishing two-mode nonclassicality correlation potentials revealing the hierarchy of the classes of single-qubit correlations in VOPS states, $\sigma(p, x)$, depending on the single-photon probability p and the coherence parameter x . Here, $x_{\max} = \sqrt{p(1-p)}$, while x_S and x_B are given in Eqs. (16) and (24), respectively.

Regime	Entanglement potential	Steering potential in three-MS	Bell nonlocality potential	Single-photon probability	Coherence parameter	Examples of states shown in figures
I	NP = 0	SP = 0	BP = 0	$p = 0$	$x = 0$	8(a)
II	NP > 0	SP = 0	BP = 0	$p \in (0, \frac{2}{3}]$	$ x \in (0, x_S]$	5(a), 6(a), 8(b), 8(c)
III	NP > 0	SP > 0	BP = 0	$p \in (0, \frac{2}{3}]$ & $p \in (\frac{2}{3}, \frac{1}{\sqrt{2}}]$	$ x \in (x_S, x_B]$ $ x \in (0, x_B]$	5(b), 5(d), 6(b) 8(e)
IV	NP > 0	SP > 0	BP > 0	$p \in (0, \frac{1}{\sqrt{2}}]$ & $p \in (\frac{1}{\sqrt{2}}, 1]$	$ x \in (x_B, x_{\max}]$ $ x \in (0, x_{\max}]$	5(c), 8(d) 5(e), 5(f), 8(f)

given in terms $\Theta(x) \equiv \max(x, 0)$, $\lambda_j^2 = \text{eig}[\rho_{\text{out}}(\sigma_2 \otimes \sigma_2)\rho_{\text{out}}^*(\sigma_2 \otimes \sigma_2)]_j$, σ_2 is a Pauli operator, and asterisk denotes complex conjugation. The concurrence is a monotone of the entanglement of formation [15]. As shown in [35], the concurrence of $\rho(p, x)$ is given simply by the single-photon probability p and the coherence parameter x ,

$$\text{CP}[\sigma(p, x)] = E[\rho(p, x)] = p. \quad (6)$$

Thus, a single-qubit state $\sigma(p, x)$ has a nonzero entanglement potential, $\text{CP}[\sigma(p, x)] > 0$ for any $p > 0$ and $|x| \in [0, \sqrt{p(1-p)}]$, i.e., for all allowed values of the parameters except $p = x = 0$.

In addition to the concurrence, one can apply the negativity, which is arguably the most popular measure of entanglement. The negativity for two qubits in a state ρ_{out} is defined by [15]:

$$N(\rho_{\text{out}}) = \max[0, -2 \min \text{eig}(\rho_{\text{out}}^\Gamma)], \quad (7)$$

where ρ_{out}^Γ is the partial transpose of ρ_{out} with respect to either qubit. Thus, the negativity potential (NP) of a single-qubit state σ is defined as the negativity N of the two-qubit output state ρ_{out} , i.e.,

$$\text{NP}(\sigma) = N(\rho_{\text{out}}). \quad (8)$$

The explicit formula for NP for an arbitrary single-qubit state $\sigma(p, x)$ reads [35]:

$$\text{NP}[\sigma(p, x)] = \frac{1}{3} \left[2\text{Re} \left(\sqrt[3]{2\sqrt{a_1} + 2a_2} \right) + p - 2 \right], \quad (9)$$

where

$$\begin{aligned} a_1 &= a_2^2 - 2[5(p-1)p + 6|x|^2 + 2]^3, \\ a_2 &= 14p^3 - 21p^2 + 15p + 9(p-2)|x|^2 - 4, \end{aligned} \quad (10)$$

which depends, in general, on the absolute value of the coherence parameter, $|x|$, which is not the case for the concurrence potential. Note that $\text{NP}[\sigma(p, x)] > 0$ iff $\text{CP}[\sigma(p, x)] > 0$, because the negativity and concurrence are good measures of two-qubit entanglement. For some

classes of states, including pure states and Werner states, $\text{NP}[\sigma(p, x)]$ and $\text{CP}[\sigma(p, x)]$ are the same, although they are different in general.

An entanglement potential can also be defined via the relative entropy of entanglement (REE) [15], as studied in, e.g., Refs. [34, 35, 40]. Unfortunately, no analytical formulas are known for the REE of $\rho(p, x)$ assuming general parameters p and x , so here we limit our study of entanglement potentials to the CP and NP.

B. Ideal steering potentials for a single qubit

EPR steering is a type of quantum nonlocality between two parties (qubits or modes) that is in general distinct from both entanglement and Bell nonlocality. In the original meaning, it describes the ability of one observer to influence another party's (qubit's) state via local measurements on its system (qubit). According to Ref. [57], EPR steering arises from the quantum correlations exhibited by quantum systems, enabling the verification of entanglement even when complete characterization of one of the subsystems is lacking. Thus, EPR steering can be interpreted as a stronger form of entanglement such that can be detected even by untrusted detectors in one subsystem. Specifically, by considering the setup shown in Fig. 1(a), this interpretation could correspond to assuming low- (high-) quality detectors used by, e.g., Alice (Bob) for their homodyne QST. Inspired by this interpretation, applications of quantum steering have been found for quantum cryptography [17] and enhanced metrology [58, 59]. Moreover, temporal [60, 61] and spatiotemporal [62] analogues of standard (spatial) quantum steering have also been found and applied in quantum cryptography [63], as well as for quantifying non-Markovianity [64], or witnessing quantum scrambling [65] and nonclassical correlations in quantum networks [62].

Here, inspired by Ref. [34] entanglement potential for a single optical mode defined via a two-mode entanglement measure, we propose to define a steering potential for a single optical qubit (or mode) quantified by a measure of standard two-qubit (or two-mode) EPR steering. In the following, for simplicity, we consider the standard

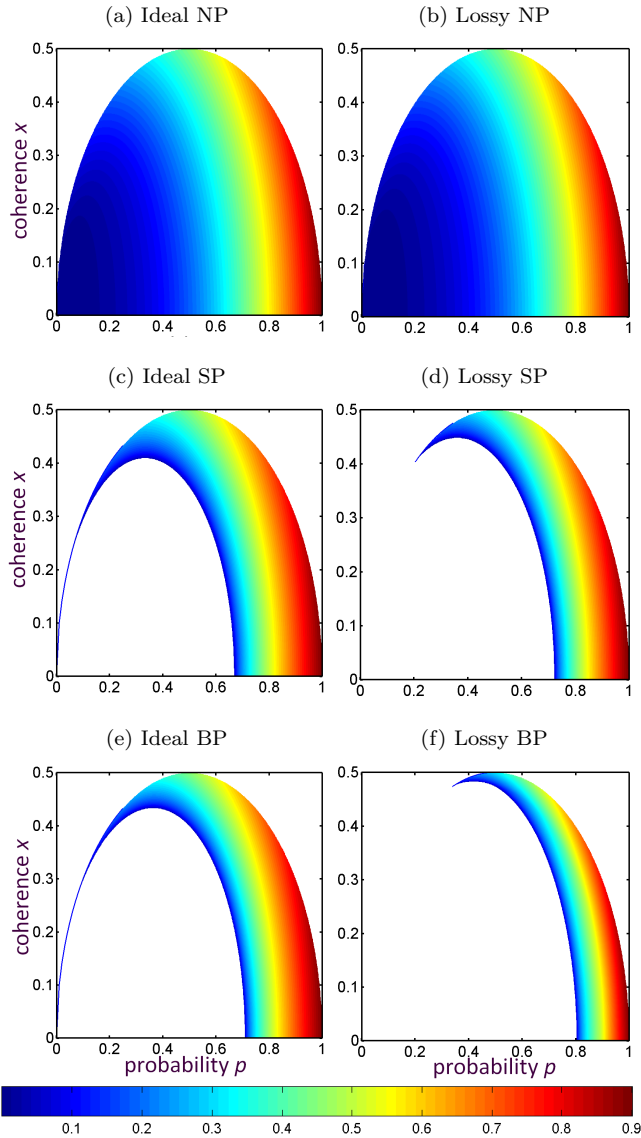


FIG. 2. Ideal and imperfect nonclassicality potentials for VOPS states $\sigma(p, x)$ showing the effects of phase damping and unbalanced BS for: $q = 0$, $r = 1/\sqrt{2}$ (first column) and $q = 0.1$, $r^2 = 0.6$ (second column): (a,b) negativity potentials NP_{qr} , (c,d) steering potentials SP_{qr} , and (e,f) Bell nonlocality potentials BP_{qr} . It is seen that these imperfections have the smallest effect on NP_{qr} and the largest effect on BP_{qr} . In panels: (a,b,c,e) the shown potentials for pure states vanish only for $p = 0$, while in (d) $SP_{qr} = 0$ for $p \in [0, 0.204]$, and in (f) $BP_{qr} = 0$ for $p \in [0, 0.339]$.

Costa-Angelo measure of steering [66] for which an analytical formula can be found. Of course, other measures of steering can also be used in defining steering potentials, including the steerable weight [67] and/or the steering robustness [68]; however, such definitions would be based on numerical calculations for general single-qubit states except some simple classes of states.

The steering potential quantified by the Costa-Angelo measure of steering [66] in a three-measurement scenario

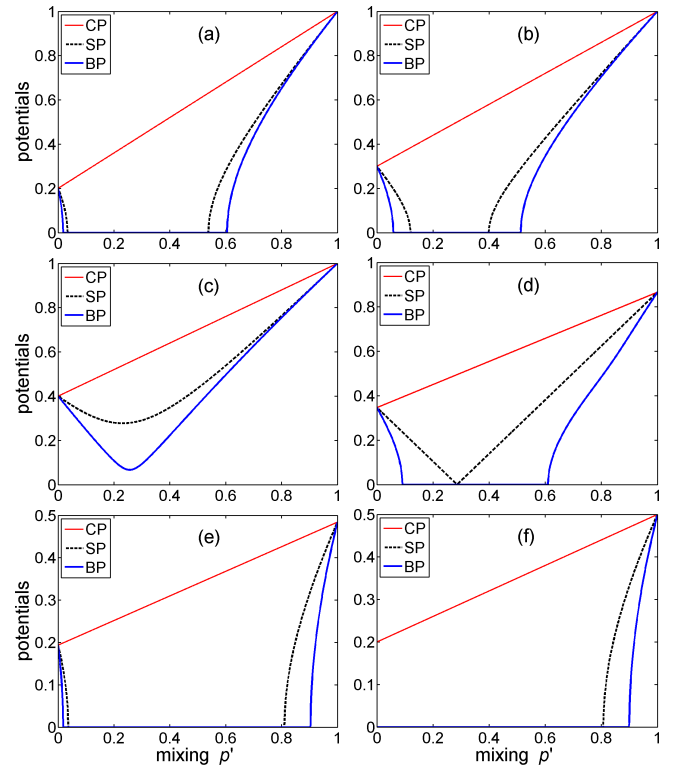


FIG. 3. Effect of mixing two single-qubit states on NC potentials: Ideal (a,b,c) and lossy (d,e,f) NC potentials for single-qubit states $\sigma'(p, p')$, given in Eq. (27), versus the mixing parameter p' for chosen values of the probability p equal to: (a) 0.2, (b) 0.3, and (c-f) 0.4. Unbalanced BS is assumed only in: (d) for $r = 1/2$, and (e) for $r = 1/4$. Phase damping with $q = 1/2$ is only assumed in (f). Graphically, the states $\sigma'(p, p')$ lie on the cross sections of Figs. 4(a,b,e) connecting the points $(p, x) = (1, 0)$ and $(p, \sqrt{p(1-p)})$, for fixed values of p .

(three-MS), corresponding to measuring the three Pauli operators on qubits of both parties, can be defined as

$$SP'(\sigma) = S_{CA}^{(3)}(\rho) = \frac{\Theta(\sqrt{\text{Tr}R} - 1)}{\sqrt{3} - 1}, \quad (11)$$

given in terms of the correlation function $R = T^T T$, where the elements of the matrix T are the two-qubit Stokes parameters, $T_{ij} = \text{Tr}[\rho(\sigma_i \otimes \sigma_j)]$. Note that the correlation matrix R , and thus $S_{CA}^{(3)}$, can be determined even experimentally without full QST, as recently demonstrated in [47]. To show this explicitly, we recall the Bloch representation of a general two-qubit state ρ :

$$\rho = \frac{1}{4} \left(I \otimes I + \mathbf{u} \cdot \boldsymbol{\sigma} \otimes I + I \otimes \mathbf{v} \cdot \boldsymbol{\sigma} + \sum_{n,m=1}^3 T_{nm} \sigma_n \otimes \sigma_m \right), \quad (12)$$

where $\boldsymbol{\sigma} = [\sigma_1, \sigma_2, \sigma_3]$ are the Pauli matrices. Moreover in Eq. (12), the elements of the Bloch vectors $\mathbf{u} = [u_1, u_2, u_3]$ and $\mathbf{v} = [v_1, v_2, v_3]$ are $u_i = \text{Tr}[\rho(\sigma_i \otimes I)]$

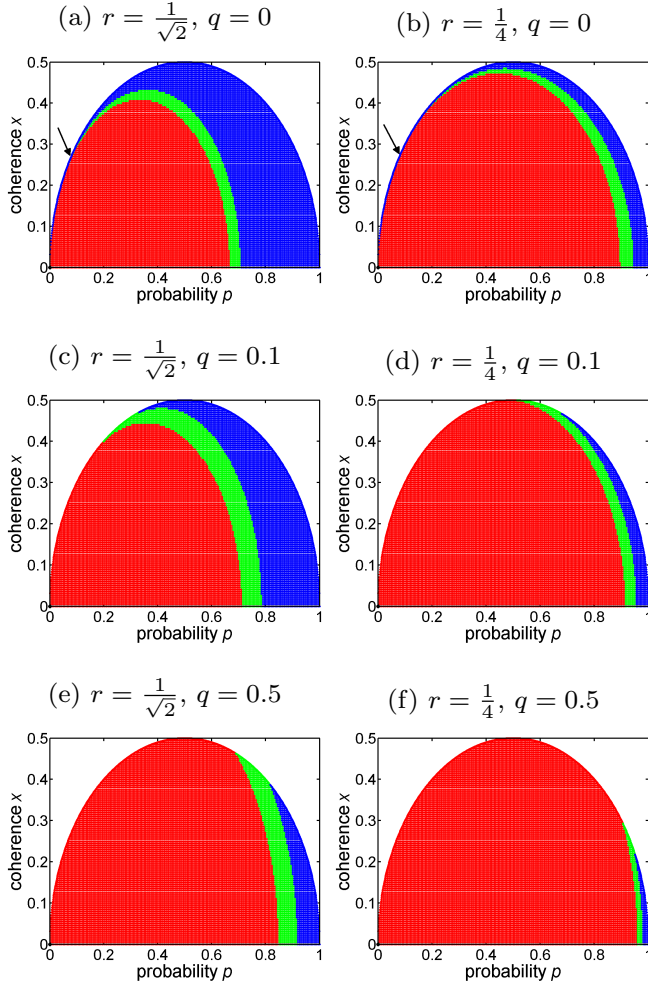


FIG. 4. Hierarchy of quantum correlations of VOPS states $\sigma(p, x)$ versus probability $p = \langle 1|\sigma|1\rangle$ and coherence parameter $|x| = |\langle 0|\sigma|1\rangle| \in [0, \sqrt{p(1-p)}]$ for given values of the beam-splitter reflection (r) and dephasing (q) parameters. Red, green, and blue regions mark the states for which it holds: (i) $\text{BP} = 0, \text{SP} = 0, \text{CP} > 0$; (ii) $\text{BP} = 0, \text{SP} > 0, \text{CP} > 0$; and (iii) $\text{BP} > 0, \text{SP} > 0, \text{CP} > 0$, respectively. The only VOPS state with $\text{BP} = \text{SP} = \text{CP} = 0$ is for $p = x = 0$. The arrows in (a,b) indicate pure states for which $\text{BP} = \text{SP} = \text{CP} > 0$, except for one point. Note that the transitions between the three regimes occur in panel (a) at $p = 2/3$ and $1/\sqrt{2}$, if $x = 0$.

and $v_i = \text{Tr}[\rho(I \otimes \sigma_i)]$, respectively, and I is the single-qubit identity operator. Thus, the reconstruction of the correlation matrix $R = T^T T$ of ρ , without reconstructing the Bloch vectors \mathbf{u} and \mathbf{v} , enables the calculation of the steering and nonlocality measures and, thus, the corresponding potentials discussed below.

The steering potential can be defined in a modified way:

$$\text{SP}(\sigma) = S^{(3)}(\rho) = \sqrt{\frac{1}{2}\Theta(\text{Tr}R - 1)}, \quad (13)$$

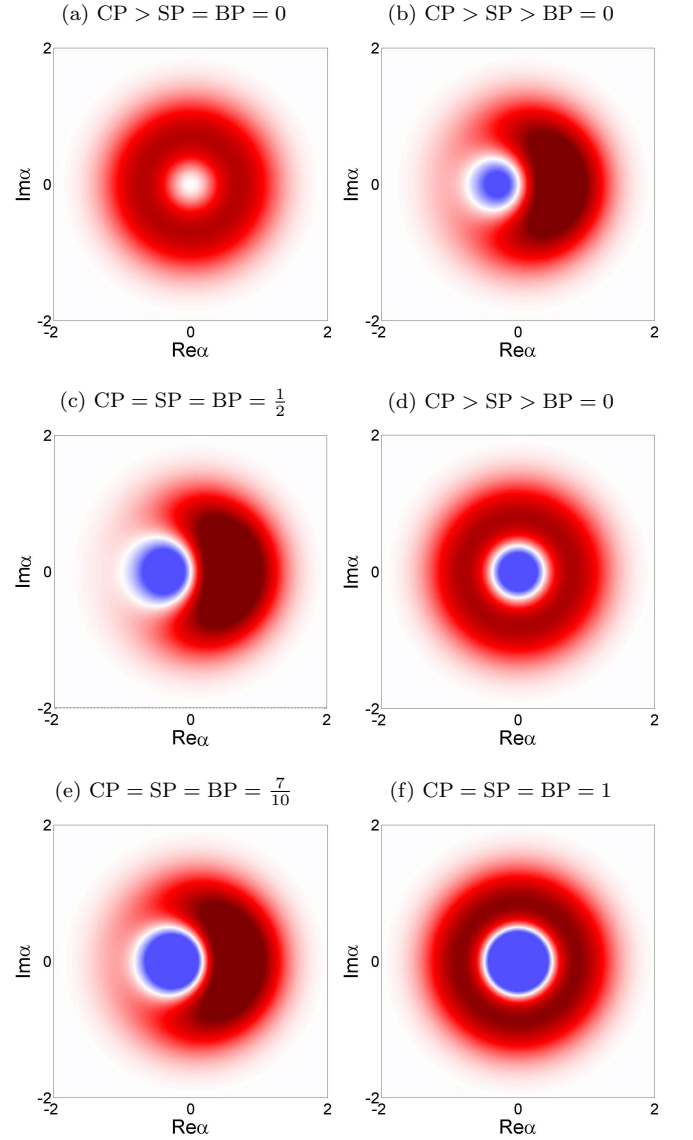


FIG. 5. Wigner functions $W(\alpha)$ for single-qubit states $\sigma(p, x)$, for chosen values of the single-photon probability p and the coherence parameter x showing the hierarchy of potentials for quantum correlations, which are summarized in Table I. Wigner functions for: (a) $\sigma(0.5, 0)$, (b) $\sigma(0.5, 0.37)$, (c) $\sigma(0.5, 0.5)$, (d) $\sigma(0.7, 0)$, (e) $\sigma[p, \sqrt{p(1-p)}]$ with $p = 0.7$, and (f) $\sigma(1, 0)$. The darker red, the larger positive values of the Wigner functions; while the darker blue, the more negative values; white color corresponds to $W(\alpha) = 0$. $W(\alpha)$ varies in the ranges: (a) $[0, 0.23]$, (b) $[-0.14, 0.50]$, (c) $[-0.23, 0.60]$, (d) $[-0.25, 0.25]$, (e) $[-0.39, 0.54]$, and (f) $[-0.64, 0.28]$. The negative regions (marked by blue) of the Wigner functions clearly show the nonclassicality of the represented states. Note that the state shown in (a) is nonclassical, although its Wigner function is nonnegative. We did not show here the trivial case of the Gaussian Wigner function for the vacuum state when $\text{CP} = \text{SP} = \text{BP} = 0$.

which corresponds to the three-MS steering measure ap-

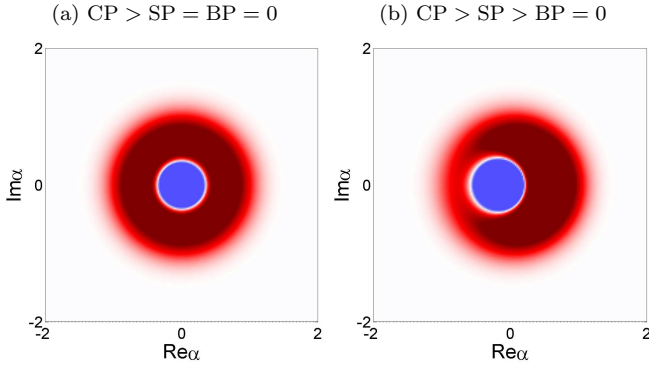


FIG. 6. Cahill-Glauber function $W^{(1/2)}(\alpha)$ for the single-qubit states (a) $\sigma(0.5, 0)$ and (b) $\sigma(0.5, 0.37)$ revealing the hierarchy of NC potentials. The states are the same as in the corresponding panels (a,b) in Fig. 5 for the Wigner function $W^{(0)}(\alpha)$. $W^{(1/2)}(\alpha)$ changes over the ranges: (a) $[-1.27, 0.57]$ and (b) $[-1.49, 1.17]$, which correspond, respectively, to the ranges: (a) $[0, 0.23]$ and (b) $[-0.14, 0.50]$ for $W^{(0)}(\alpha)$. The negative values of $W^{(1/2)}(\alpha)$ clearly show the NC character of the states, even if the corresponding $W^{(0)}(\alpha)$ is nonnegative in the entire phase space.

plied in Refs. [47, 69, 70]). Note that $S_{CA}^{(3)}$ and $S^{(3)}$ are both measures of the violation of the steering inequality derived by Cavalcanti, Jones, Wiseman, and Reid (CJWR) in the three-MS [71]. The two steering potentials are monotonically related for arbitrary single-qubit states σ by

$$SP'(\sigma) = \frac{\sqrt{2[SP(\sigma)]^2 + 1} - 1}{\sqrt{3} - 1} \leq SP(\sigma). \quad (14)$$

in analogy to the corresponding relation for the steering measures [47]. In this paper we focus on $SP(\sigma)$ because it reduces to the entanglement potential for any two-qubit pure states, $\sigma[p, \sqrt{p(1-p)}] \equiv |\psi\rangle\langle\psi|$. On the other hand, $SP'(\sigma)$ calculated for experimentally reconstructed states gives usually a better agreement with theoretical predictions (see Ref. [47] for comparison of experimentally determined $S_{CA}^{(3)}$ and $S^{(3)}$ for Werner-like states). Thus, we present both definitions.

We find that the steering potential in the three-MS for a single-qubit state $\sigma(p, x)$ is given by

$$SP(\sigma) = \sqrt{\Theta(3p^2 - 2p + 2|x|^2)}, \quad (15)$$

clearly depending on the coherence parameter $|x|$, which is not the case for $CP(\sigma)$. Thus, we find that a given state $\sigma(p, x)$ has a nonzero steering potential, $SP[\sigma(p, x)] > 0$ for: (i) $p \in (0, 2/3]$ if $|x| \in (x_S(p), \sqrt{p(1-p)}]$, where

$$x_S(p) = \sqrt{p(1 - 3p/2)}, \quad (16)$$

and (ii) $p \in (2/3, 1]$ if $|x| \in [0, \sqrt{p(1-p)}]$.

To explain a rapid decrease and vanishing of the SP by introducing even a slight decoherence of a pure state

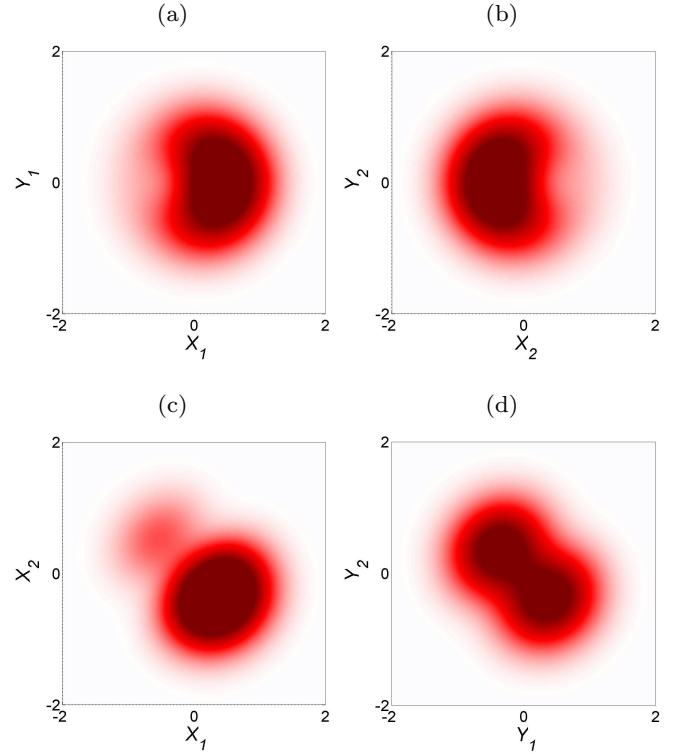


FIG. 7. Marginal distributions of two-mode Wigner functions $W(\alpha_1, \alpha_2)$, i.e.: (a) $W(X_1, Y_1)$, (b) $W(X_2, Y_2)$, (c) $W(X_1, X_2)$, and (d) $W(Y_1, Y_2)$, where $X_i = \text{Re}(\alpha_i)$ and $Y_i = \text{Im}(\alpha_i)$, for single-photon two-mode states $\rho(p, x)$ assuming $p = 0.5$ and $x = 0.37$. This state is steerable in the three-MS, but Bell local (so unsteerable in the two-MS), and it corresponds to $\sigma(p, x)$ shown in Fig. 5(b). The maximum values of these non-negative Wigner functions are: (a,b) 0.50, (c) 0.67, and (d) 0.39.

$\sigma[p, \sqrt{p(1-p)}]$ for small p , as seen in Figs. 2(c), 3(a), and 3(b), we introduce a decoherence factor $\kappa \in [0, 1]$, such that $x = \kappa\sqrt{p(1-p)}$. By analyzing Eq. (15), one readily finds that the decoherence factor should satisfy

$$\kappa > \kappa_0 = \frac{2 - 3p}{2 - 2p}, \quad (17)$$

to guarantee that $SP(\sigma) > 0$. Thus, we see that the steering potential is nonzero for any value of κ (and so x) if $p > 2/3$. However, if $p = 0.1$ (0.2), $SP(\sigma) > 0$ for $\kappa > 0.94$ (> 0.875). This clearly explains a rapid disappearance of the steering potential shown by the thin curve on the left-hand side of Fig. 2(c). Moreover, even a more rapid loss of the nonlocality potential can be seen in Fig. 2(e), because a vanishing SP implies a vanishing BP.

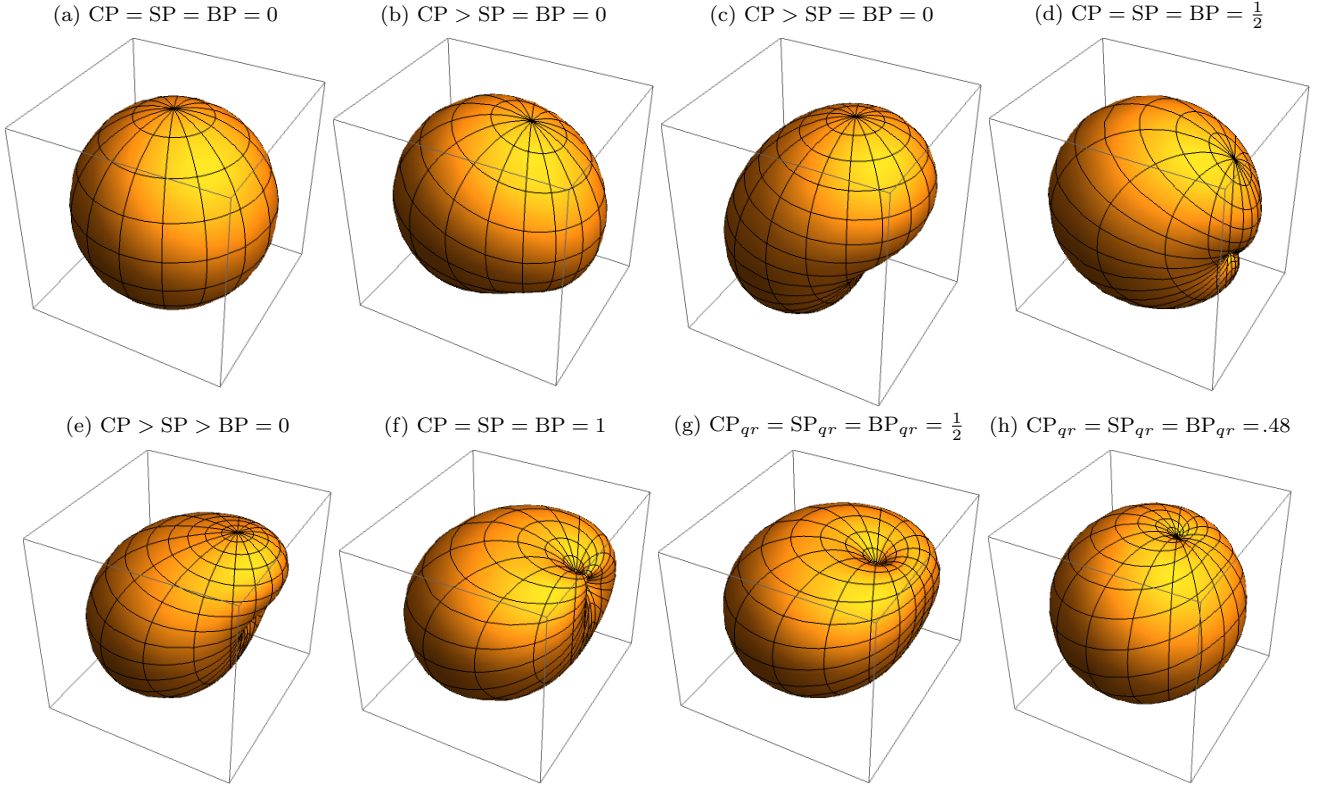


FIG. 8. Angular-momentum probability surfaces (AMPSs) for chosen two-mode states $\rho_{qr}(p, x)$, given in Eq. (30) corresponding to a qutrit, revealing the hierarchy of the ideal (a-f) and lossy (g,h) potentials for entanglement (CP and CP_{qr}), steering (SP and SP_{qr}), and Bell nonlocality (BP and BP_{qr}), respectively. In the ideal cases the BS is balanced ($r = 1/\sqrt{2}$) and no phase damping occurs ($q = 0$); while for the non-ideal cases we set: (g) phase damping with $q = 1/2$ for a balanced BS; and (h) unbalanced BS with $r = 1/4$ and no phase damping. The chosen two-mode states are: (a) $\rho(0, 0) = |0\rangle\langle 0|$, (b) $\rho(0.1, 0)$, (c) $\rho(\frac{1}{2}, 0)$, (d) $\rho(\frac{1}{2}, \frac{1}{2})$, (e) $\rho(0.7, 0)$, and (f,g,h) $\rho(1, 0) = |1\rangle\langle 1|$. In (h), a more precise value of the three potentials is 0.4841.

C. Bell nonlocality potentials for a single qubit

Single-qubit Bell nonlocality potentials can be introduced via Bell nonlocality measures of a given two-qubit state ρ quantifying the violation of the Bell inequality in the Clauser-Horne-Shimony-Holt form (denoted as Bell-CHSH) [72]:

$$|\langle \mathcal{B} \rangle_\rho| \equiv |\langle \mathbf{a} \cdot \boldsymbol{\sigma} \otimes (\mathbf{b} + \mathbf{b}') \cdot \boldsymbol{\sigma} + \mathbf{a}' \cdot \boldsymbol{\sigma} \otimes (\mathbf{b} - \mathbf{b}') \cdot \boldsymbol{\sigma} \rangle_\rho| \leq 2, \quad (18)$$

given in terms of the Bell-CHSH operator \mathcal{B} , where $\mathbf{a}, \mathbf{a}', \mathbf{b}, \mathbf{b}' \in \mathbb{R}^3$ are unit vectors describing measurement settings. As described by Horodecki *et al.* [73], the maximum possible violation of the Bell-CHSH inequality in Eq. (18) considered over all measurement settings, can be used as a Bell nonlocality measure, i.e., $\max_{\nu} \langle \mathcal{B} \rangle_\rho = 2\sqrt{\mathcal{M}(\rho)}$, where $\mathcal{M}(\rho)$ is the sum of the two largest eigenvalues of the correlation matrix $R(\rho)$. The Bell-CHSH inequality is satisfied if and only if $\mathcal{M}(\rho) \leq 1$. To make our comparison of various types of quantum correlations consistent, as based on measures and potentials defined in the range $[0, 1]$, the Bell nonlocality measure of Ref. [73] is often rescaled as $B(\rho) = \sqrt{\Theta[\mathcal{M}(\rho) - 1]}$ (see,

e.g., Refs. [70, 74, 75]). Thus, we define a Bell nonlocality potential as

$$\begin{aligned} \text{BP}(\sigma) &= B(\rho) = \sqrt{\Theta[\mathcal{M}(\rho) - 1]} \\ &= \sqrt{\Theta\{\text{Tr}R - \min[\text{eig}(R)] - 1\}}. \end{aligned} \quad (19)$$

This measure is monotonically related to the Costa-Angelo measure of steering [66] defined in the two-measurement scenario (two-MS), which corresponds to measuring two Pauli operators on qubits of both parties [66]. Specifically, the related nonlocality potential reads

$$\text{BP}'(\sigma) = S_{\text{CA}}^{(2)}(\rho) = \frac{\Theta\{\sqrt{\text{Tr}R - \min[\text{eig}(R)]} - 1\}}{\sqrt{2} - 1}, \quad (20)$$

which is simply related to $\text{BP}(\sigma)$ as

$$\text{BP}'(\sigma) = \frac{\sqrt{[\text{BP}(\sigma)]^2 + 1} - 1}{\sqrt{2} - 1} \leq \text{BP}(\sigma). \quad (21)$$

Note that $B, B', BP, BP' \in [0, 1]$ for arbitrary two-qubit states. We find that

$$\begin{aligned} \min[\text{eig}(R)] &= \frac{1}{2} \left(1 + p(5p - 4) + 4|x|^2 \right. \\ &\quad \left. - (1 - p)\sqrt{(1 - 3p)^2 + 8|x|^2} \right), \\ \text{Tr}R &= 1 - 4p + 6p^2 + 4x^2, \end{aligned} \quad (22)$$

so the Bell nonlocality potential BP for a general state $\sigma(p, x)$ with $p \in [0, 1]$ and $x \in [0, \sqrt{p(1-p)}]$ becomes

$$\text{BP}[\sigma(p, x)] = \left\{ \Theta \left[\frac{1}{2} (7p^2 + (1 - p)\sqrt{(1 - 3p)^2 + 8|x|^2} - 4p + 4|x|^2 - 1) \right] \right\}^{1/2}. \quad (23)$$

We find that a given state $\sigma(p, x)$ has a nonzero nonlocality potential, $\text{BP}[\sigma(p, x)] > 0$ for: (i) $p \in (0, \frac{1}{\sqrt{2}}]$ with $|x| \in (x_B(p), \sqrt{p(1-p)})$, where

$$x_B(p) = \frac{1}{\sqrt{2}} \sqrt{1 + p - 3p^2 - (1 - p)\sqrt{1 - p^2}}, \quad (24)$$

and (ii) $p \in (\frac{1}{\sqrt{2}}, 1]$ with $|x| \in [0, \sqrt{p(1-p)}]$.

D. Hierarchy of nonclassicality potentials

Single-qubit correlations, as quantified by the NC potentials, satisfy the following hierarchy:

$$\text{BP}(\sigma) \leq \text{SP}(\sigma) \leq \text{NP}(\sigma) \leq \text{CP}(\sigma), \quad (25)$$

for an arbitrary state $\sigma(p, x)$. This hierarchy is in close analogy to that for the corresponding two-qubit correlation measures (see, e.g., [47]). For single-qubit pure states $\sigma(p, \sqrt{p(1-p)}) = |\psi\rangle\langle\psi|$, the potentials become the same,

$$\text{BP}(|\psi\rangle) = \text{SP}(|\psi\rangle) = \text{NP}(|\psi\rangle) = \text{CP}(|\psi\rangle) = p. \quad (26)$$

Figure 4(a) shows the hierarchy of ideal NC potentials, i.e., assuming a lossless and balanced BS. In addition to the vacuum (for $p = x = 0$), which is the only separable VOPS state, this hierarchy includes the states with the potentials for: (i) non-steerable entangled states (corresponding to the red region), (ii) steerable states but Bell local (in the green region), and (iii) Bell nonlocal states (in the blue region). We can see in this figure that a VOPS state has nonvanishing SP or BP if either p is sufficiently large (and then independent of x) or if smaller values of p are accompanied by a sufficiently large x . The same conclusion can be drawn by analyzing Figs. 2(c,e) and Eqs. (16), (17), and (24).

Figures 3(a,b,c) show the ideal NC potentials and their hierarchy for the mixed states defined as

$$\sigma'(p, p') = p'|1\rangle\langle 1| + (1 - p')|\psi_p\rangle\langle\psi_p|, \quad (27)$$

where $|\psi_p\rangle = \sqrt{p}|1\rangle + \sqrt{1-p}|0\rangle$. These states lie on the cross sections of some graphs in Fig. 4 as explained in detail in the caption of Fig. 3. In particular, a very narrow region, which close to $p' = 0$ with nonzero BP and SP, is shown in Fig. 3(a) for $p = 0.2$.

III. REALISTIC NONCLASSICALITY POTENTIALS

We stress that the standard entanglement potentials of Ref. [34] are based solely on the special case of ρ_{out} for a balanced (50/50) BS assuming no dissipation. Now we analyze how experimental imperfections can affect the two-qubit states generated from single-qubit states given in Eq. (1).

We first consider the effect of phase damping. Specifically, the Kraus operators for a single-qubit phase-damping channel (PDC) read [76]:

$$E_0(q_i) = |0\rangle\langle 0| + \sqrt{1 - q_i}|1\rangle\langle 1|, \quad E_1(q_i) = \sqrt{q_i}|1\rangle\langle 1|, \quad (28)$$

where q_i (with $i = 1, 2$) are phase-damping coefficients (rates), and the Kraus operators satisfy the normalization relation $\sum_{n=0,1} E_n^\dagger(q_i)E_n(q_i) = I$. Two-qubit phase damping transforms a given two-mode state ρ_{in} to

$$\rho_{\text{PDC}} = \sum_{i,j} [E_i(q_1) \otimes E_j(q_2)] \rho_{\text{in}} [E_i^\dagger(q_1) \otimes E_j^\dagger(q_2)]. \quad (29)$$

For simplicity, we analyze the same phase damping rate in both qubits, so we set $q \equiv q_1 = q_2$.

We also consider the effect of an unbalanced BS on the generation of two-mode states, as given by Eq. (2) for $r \neq t = \sqrt{1 - r^2}$. By the inclusion of these effects, we find that the output state ρ_{out} , given in Eq. (2), now generalizes to

$$\rho_{qr}(p, x) = \begin{bmatrix} 1 - p & -Qrx & Qtx & 0 \\ -Qrx^* & pr^2 & -pQ^2rt & 0 \\ Qtx^* & -pQ^2rt & pt^2 & 0 \\ 0 & 0 & 0 & 0 \end{bmatrix}, \quad (30)$$

where $Q = \sqrt{1 - q}$ for the phase damping parameter q . Equation (30) reduces to Eq. (3) for $r = t = 1/\sqrt{2}$ and $q = 0$.

Thus, by considering these imperfections, we can analyze the entanglement, steering, and Bell nonlocality generalized potentials corresponding to more realistic experimental situations, as defined, respectively, by

$$\text{CP}_{qr}(\sigma) = C(\rho_{qr}), \quad (31)$$

$$\text{NP}_{qr}(\sigma) = N(\rho_{qr}), \quad (32)$$

$$\text{SP}_{qr}(\sigma) = S^{(3)}(\rho_{qr}), \quad (33)$$

$$\text{BP}_{qr}(\sigma) = B(\rho_{qr}), \quad (34)$$

and analogously to the related potentials based on $S_{\text{CA}}^{(3)}(\rho_{qr})$ and $S_{\text{CA}}^{(2)}(\rho_{qr})$. The hierarchy relations, given

in Eq. (25) for the ideal potentials, simply generalize for the realistic (i.e., lossy) NC potentials to

$$\text{BP}_{qr}(\sigma) \leq \text{SP}_{qr}(\sigma) \leq \text{NP}_{qr}(\sigma) \leq \text{CP}_{qr}(\sigma). \quad (35)$$

We find that the concurrence generalized potential reads

$$\text{CP}_{qr}[\sigma(p, x)] = C[\rho_{qr}(p, x)] = 2p(1-q)rt = p(1-q) \sin \theta, \quad (36)$$

where the BS parameter θ is defined below Eq. (2). One can define other entanglement generalized potentials based on, e.g., the universal witness of entanglement (UWE) can be defined by $\det \rho^\Gamma$ [77] or $\Theta(-\det \rho^\Gamma)$ to be consistent with the definitions of other nonclassicality quantifiers applied in this paper. Note that an effective experimental method for measuring the UWE without full QST was described in [78] (although the method has not been implemented experimentally yet). The measurement of the concurrence of a two-qubit state requires usually its full QST. The UWE and the corresponding entanglement generalized potential UWEP_{qr} for the θ -dependent BS output state reads

$$\text{UWEP}_{qr} \equiv \Theta[-\det \rho_{qr}^\Gamma(p, x)] = (\frac{1}{2}p \sin \theta)^4 (1-q)^2, \quad (37)$$

being independent of x , which is the same as for the concurrence potential CP_{qr} , but contrary to the negativity potential NP_{qr} . Anyway, it holds

$$\text{UWEP}_{qr}(\sigma) > 0 \Leftrightarrow \text{CP}_{qr}(\sigma) > 0 \Leftrightarrow \text{NP}_{qr}(\sigma) > 0, \quad (38)$$

for any x . Note that the analytical expression for NP_{qr} , which generalizes Eq. (9), is quite lengthy, so it is not presented here.

We stress that all the nonclassicality measures and quantifiers considered in this paper, are independent of the phase of x , although the R matrix depends. So, to have compact formulas for the R matrix, let us set in the following equations that the coherence parameter x is real. Then the correlation matrix R reads

$$R = \begin{bmatrix} 4Zp^2 + 4Q^2r^2x^2 & 0 & Y \\ 0 & 4p^2Z & 0 \\ Y & 0 & (1-2p)^2 + 4Q^2t^2x^2 \end{bmatrix}, \quad (39)$$

where

$$\begin{aligned} Y &= 2Qr(-2pQ^2t^2 + 2p - 1)x, \\ Z &= Q^4r^2t^2 = \frac{1}{4}(1-q)^2 \sin^2 \theta. \end{aligned} \quad (40)$$

The eigenvalues of R are found as:

$$\begin{aligned} e_{1,2} &= \frac{1}{2} \left(1 + 4 [Q^2x^2 + p^2(Z+1) - p] \pm \sqrt{f_e} \right), \\ e_3 &= 4p^2Z = [p(1-q) \sin \theta]^2, \end{aligned} \quad (41)$$

where

$$f_e = (\text{Tr}R - 4p^2Z)^2 - 16Z(2p^2 + 2x^2 - p)^2. \quad (42)$$

Thus, we have

$$\begin{aligned} \text{Tr}R &= \sum e_i = 4p(2pZ + p - 1) + 4Q^2x^2 + 1, \quad (43) \\ \min[\text{eig}(R)] &= \min(e_2, e_3), \quad (44) \end{aligned}$$

which enable the calculation of the generalized potentials for SP_{qr} and BP_{qr} .

The hierarchy of the lossy NC potentials is plotted in Figs. 4(b-f) in comparison to the ideal NC potentials shown in Fig. 4(a). The red, green, and blue regions show, respectively, the regimes II, III, and IV listed in Table I; while the point $(p, x) = (0, 0)$ indicates the only separable VOPS state (i.e., the vacuum), which belongs to the regime I. It is clearly seen that dephasing and unbalanced beam splitting considerably decrease the regions of the nonvanishing steering and nonlocality potentials.

IV. PHASE-SPACE AND ANGULAR-MOMENTUM DESCRIPTIONS OF NONCLASSICALITY

A. Wigner and Cahill-Glauber quasiprobability distributions

To visualize the nonclassicality of the analyzed single- and two-mode states, we here apply the standard Wigner functions and their generalizations.

It is well known that linear transformations (including that of a BS) do not change the global nonclassicality of states. This can be convincingly demonstrated using the Cahill-Glauber s -parametrized quasiprobability distribution (QPD), which is defined for any $s \in [-1, 1]$ in Appendix A. Note that the s -parametrized QPD reduces in special cases to the standard Wigner ($W = \mathcal{W}^{(0)}$) and Husimi ($W = \mathcal{W}^{(-1)}$) functions, which can be measured experimentally, and to the Glauber-Sudarshan function ($P = \mathcal{W}^{(1)}$), which is used in the definition of the nonclassicality of optical fields, but usually cannot be measured experimentally, because of its singularity (except very special nonclassical fields).

For example, a perfect BS transformation, which is given by the unitary transformation U_{BS} , given below Eq. (2), of an arbitrary input state ρ_{in} (of any dimension) resulting in the two-mode output state ρ_{out} , can equivalently be described by the evolution in a two-mode phase space of the corresponding QPD given by [79]

$$\mathcal{W}_{\text{out}}^{(s)}(\alpha_1, \alpha_2) = \mathcal{W}_{\text{in}}^{(s)}(t\alpha_1 + r\alpha_2, r\alpha_1 - t\alpha_2). \quad (45)$$

This equation implies that the initial QPD is displaced, without changing its form, along a trajectory in the phase space spanned by the canonical position ($X_i \equiv \text{Re } \alpha_i$ for $i = 1, 2$) and ($Y_i \equiv \text{Im } \alpha_i$) momentum operators. The trajectory is given by the solution of the corresponding classical equations of motion. Thus, the global nonclassicality of the state is unchanged during this evolution.

In this paper we are mainly interested in a special case of the BS transformation assuming a VOPS state σ in one input ports and the vacuum in another port. Then, Eq. (45) reduces to

$$\mathcal{W}_{\text{out}}^{(s)}(\alpha_1, \alpha_2) = \mathcal{W}_{\text{vops}}^{(s)}(t\alpha_1 + r\alpha_2) \mathcal{W}_{\text{vac}}^{(s)}(r\alpha_1 - t\alpha_2), \quad (46)$$

where $\mathcal{W}_{\text{vac}}^{(s)}$ is the single-mode-vacuum QPD given by

$$\mathcal{W}_{\text{vac}}^{(s)}(\alpha) = \frac{1}{\pi} T_{00}^{(s)}(\alpha) = \frac{2}{\pi(1-s)} \exp\left(-\frac{2}{1-s}|\alpha|^2\right), \quad (47)$$

and $\mathcal{W}_{\text{vops}}^{(s)}(\alpha)$ is the QPD for an arbitrary single-mode state $\sigma(p, x)$:

$$\mathcal{W}_{\text{vops}}^{(s)}(\alpha) = \frac{1}{\pi} \left[(1-p)T_{00}^{(s)}(\alpha) + pT_{11}^{(s)}(\alpha) + xT_{10}^{(s)}(\alpha) + x^*T_{01}^{(s)}(\alpha) \right], \quad (48)$$

with the functions $T_{nm}^{(s)}(\alpha)$ given explicitly in Eq. (A9). Note that Eq. (47) is a special case of Eq. (48). Another important special case of that formula is the QPD $\mathcal{W}_{1\text{ph}}^{(s)}(\alpha) = T_{11}^{(s)}(\alpha)/\pi$ for the single-photon Fock state:

$$\mathcal{W}_{1\text{ph}}^{(s)}(\alpha) = \frac{2(4|\alpha|^2 + s^2 - 1)}{\pi(1-s)^3} \exp\left(-\frac{2}{1-s}|\alpha|^2\right), \quad (49)$$

which in the limit $s \rightarrow 1$ becomes a derivative of Dirac's δ -function [14]:

$$P_{1\text{ph}}(\alpha) \equiv \mathcal{W}_{1\text{ph}}^{(1)}(\alpha) = \left(1 + \frac{\partial}{\partial\alpha} \frac{\partial}{\partial\alpha^*}\right) \delta(\alpha), \quad (50)$$

which can be easily shown by representing $\delta(\alpha)$ as the limit of the sequence of zero-centered normal distributions, i.e., $\mathcal{W}_{\text{vac}}^{(s)}(\alpha)$. Equation (50), and thus also Eq. (48) for $s = 1$, clearly show a nonclassical character of any VOPS state (except the vacuum), as these P -functions are more singular than that for a coherent state $|\alpha\rangle$, i.e., $P_{\text{coh}}(\alpha) = \delta(\alpha)$.

The Wigner function for an arbitrary VOPS state $\sigma(p, x)$, which can be obtained from Eq. (48), reads

$$W_{\text{vops}}(\alpha) = \frac{2}{\pi} \left[(1-p) + p(4|\alpha|^2 - 1) + 2\text{Re}(x\alpha) \right] \exp(-2|\alpha|^2). \quad (51)$$

Examples of the single-mode Wigner and Cahill-Glauber distribution for a chosen σ state are plotted in Figs. 5 and 6, respectively.

Experimentally reconstructed two-mode Wigner functions $W(\alpha_1, \alpha_2)$ are usually shown graphically (see, e.g., [80]) via their marginal functions of four different quadrature pairs, i.e.: $W(X_1, X_2) = \int W(\alpha_1, \alpha_2) dY_1 dY_2$, and analogously $W(Y_1, Y_2)$, $W(X_1, Y_1)$, and $W(Y_2, X_2)$. As an example, we show such four marginal distributions in Fig. 7 for $\rho(p = 0.5, x = 0.37)$.

The Cahill-Glauber QPD, $W^{(1/2)}(\alpha)$, was calculated using Eq. (A7), while the Wigner functions were calculated from: (i) the simple formulas in Eqs. (46), (47), and (51) for the model without phase damping, i.e., for the BS output state in Eq. (3); and (ii) the general definition of the two-mode Wigner function, given in Eq. (48), for two-mode states affected by phase damping according to Eq. (30).

B. Angular-momentum probability surfaces

Because the studied two-mode states are limited to two qubits or even formally to a single qutrit, as implied Eq. (30), we can visualize their properties more compactly using angular-momentum probability surfaces (AMPS) or, equivalently, angular-momentum Wigner functions. As defined in [81–83], an AMPS [say $\rho_{JJ}(\theta, \phi)$] for a given $(2J+1) \times (2J+1)$ state ρ (which can be interpreted as an angular-momentum state for any J) is a three-dimensional closed surface, where the distance from the origin in a specific direction corresponds to the probability of the maximum projection of ρ along that direction. An AMPS $\rho_{JJ}(\theta, \phi)$ can be given as a linear combination of spherical harmonics with the coefficients corresponding to the moments of a polarization operator, and the Clebsch-Gordan coefficients (see [82] for details).

A one-to-one correspondence between a given ρ and $\rho_{JJ}(\theta, \phi)$ can be easily shown by recalling the orthonormality of the spherical harmonics. Alternatively, one can apply the angular-momentum Wigner functions introduced by Agarwal [84] (see also [85]), which are also simply related to the AMPS [83]. Thus, the AMPS, and the above-mentioned standard and generalized Wigner functions can be interchangeably used as complete representations of the studied state ρ .

In our case, we encode the Fock basis states $|00\rangle$, $|01\rangle$, and $|10\rangle$ into, respectively, the angular momentum states $|J, -1\rangle$, $|J, 0\rangle$, and $|J, 1\rangle$, where $J = 1$ corresponds to a qutrit. We note that other encodings can also be applied. We have shown in Fig. 8, the AMPS for chosen states, which reveal different relations between the NC potentials corresponding to all the hierarchy regimes listed in Table I.

V. DISCUSSION

A. Experimental feasibility

1. Generation of arbitrary vacuum-one-photon superpositions

A number of methods for generating superpositions of Fock states, including the studied VOPS states, have been proposed and implemented experimentally with optical [24, 86–89] or microwave [90] photons.

In particular, VOPS can be generated from a coherent state by generalized conditional quantum teleportation and projective synthesis using a quantum scissors device, as shown schematically in Fig. 1(b). The method was proposed in [91], its experimental feasibility was analyzed in detail in [92, 93], and it was experimentally implemented in [88]. The device comprises two balanced beam splitters BS_1 and BS_2 . A single-photon state $|1\rangle$ is mixed with the vacuum $|0\rangle$ on BS_1 , and the generated entangled state at one of the BS_1 outputs is mixed with a coherent state $|\alpha\rangle$ (with a complex amplitude α) at BS_2 . To generate a desired pure state $\sigma[p, \sqrt{p(1-p)}] = |\psi\rangle\langle\psi|$, the amplitude α should satisfy the condition $p/(1-p) = |\alpha|^2$, so $|\psi\rangle \sim (|0\rangle + \alpha|1\rangle)$. The projection synthesis of $|\psi\rangle$ is realized by conditional measurements at the two single-photon detectors, D_1 and D_2 . A proper generation of $|\psi\rangle$ at the second output port of BS_1 occurs if the detector D_1 registers a single photon and D_2 does not register any (or vice versa). In case of other measurement results, the generation (and qubit teleportation) is unsuccessful, so the procedure should be repeated. Note that a VOPS state is generated via quantum state truncation (which can be considered a measurement-induced photon blockade process) and via the conditional teleportation of the truncated state.

To generate an incoherent VOPS state $\sigma(p, x)$ with a coherence factor $|x| < \sqrt{p(1-p)}$, a phase shifter can be applied (with a specific probability), as shown in Fig. 1(b). For example, by using random 0 or π phase shifts with a given probability, one can decohere a given pure-state superposition to an arbitrary degree. A phase shifter can be replaced by two kinds of mirrors changing the phase of a state during its reflection by either 0 or π . Let us assume that the state $|\psi_0\rangle = \mathcal{N}(|0\rangle + \alpha|1\rangle)$ for $\phi = 0$ was generated n_0 times, and $|\psi_1\rangle = \mathcal{N}(|0\rangle - \alpha|1\rangle)$ for $\phi = \pi$ was produced n_1 times, where \mathcal{N} is the normalization constant. In fact, the state $|\psi_1\rangle$ is generated in the scheme if a single photon is detected by D_2 instead of D_1 ; thus, no phase shifter is required for generating $|\psi_1\rangle$. The corresponding mixed state reads $\sigma' = \sum_{i=0,1} n_i |\psi_i\rangle\langle\psi_i| / (n_0 + n_1)$; so, if $n_1 = n_0$ then $x = 0$, and if $n_1 = 0$ then $x = \sqrt{p(1-p)}$. Thus, by choosing properly n_1 compared to n_0 , one can obtain any value of $|x| \in [0, \sqrt{p(1-p)}]$.

VOPS states can also be generated conditionally (via postselection) using other linear-optical schemes, e.g., via: quantum-optical catalysis [24], spontaneous parametric down-conversion [86], or a single-photon linear amplification with finite gain [94].

We focus here on freely propagating VOPS states generated in a linear-optical system. We note that the generation and control of arbitrary superpositions of harmonic-oscillator states were experimentally demonstrated also in various other systems, which include microwave resonators [90, 95–97] and optical cavities [98], or even ion traps, where superpositions of motional states of trapped ions were generated [99]. Thus, our classification of NC is not limited to VOPS states, but also applies to other

bosonic excitations.

2. Two-mode state tomography

Once a desired VOPS state is generated, it is mixed with the vacuum on a balanced BS and then a two-mode Wigner function can be reconstructed using, e.g., homodyne QST as shown in Fig. 1(a). It should be noted that from the experimental point of view, it is much more challenging to perform optical tomography on qubit states implemented as VOPS states compared to such tomographic measurements of optical qubits implemented in other ways, including photon polarization. Anyway, a number of experiments reported the generation of VOPS states and their tomographic reconstruction via homodyne detection [24–26, 88, 89]. Homodyne tomographic measurements of the joint detection probabilities for testing Bell nonlocality were first considered on correlated optical beams at the output of a nondegenerate parametric amplifier in Ref. [100].

Thus, a typical setup of two-mode homodyne QST, as schematically shown in Fig. 1(a), can be applied for reconstructing a two-qubit Wigner function $W(\alpha_1, \alpha_2)$ from which the corresponding density matrix ρ_{exp} can be calculated by Eq. (A6). To find the corresponding single-qubit state $\sigma(p, x)$, one can numerically find the closest state $\rho_{qr}(p, x)$, given in Eq. (30), maximizing the Uhlmann-Jozsa fidelity (or, equivalently, minimizing the Bures distance),

$$\begin{aligned} F_{\text{max}} &= \max_{p,x,q,r} F[\rho_{\text{exp}}, \rho_{qr}(p, x)] \\ &\equiv \max_{p,x,q,r} \left[\text{Tr} \left(\sqrt{\sqrt{\rho_{\text{exp}}} \rho_{qr}(p, x) \sqrt{\rho_{\text{exp}}}} \right) \right]^2. \end{aligned} \quad (52)$$

Homodyne QST for reconstructing two-mode Wigner function can be replaced by the Lutterbach-Davidovich QST [101] based on performing proper displacements in a phase space and parity measurements using the Cahill-Glauber formula, given in Eq. (A6). The single-mode QST method was experimentally applied in, e.g., [90] for reconstructing single-mode Wigner functions of Fock-state superpositions (including VOPS states) in a superconducting resonator. The Lutterbach-Davidovich method can be readily applied for reconstructing also two-mode Wigner functions (as experimentally implemented in, e.g., [102]), in the same spirit as single-mode homodyne QST was generalized to two-mode QST [see Fig. 1(a)]. Moreover, a modified Lutterbach-Davidovich method can be applied for reconstructing also the single- and two-mode Cahill-Glauber s -parametrized QPDs given in Eqs. (A1) and (A4) for s not too close 1.

The NC of experimental VOPS states can be tested by applying various NC witnesses, including a Vogel criterion [14] as applied in [24], or negative Wigner functions [89]. The NC of single-photon Fock states was experimentally tested via violating a Bell inequality calculated from a two-mode density matrix reconstructed via

homodyne detection in [25, 26]; those results can be considered as a special case of our nonlocality potential for a single-photon Fock-like state generated experimentally, and other $\sigma(p, x)$ states were not studied there.

At the end of this section we would like to stress the importance of applying quantum state tomography in this study. Specifically, we are interested not only in testing whether a single-mode state exhibits a given type of quantum correlations, but our goal is to quantify the NC of the state via measures of two-mode quantum correlations, and finally to demonstrate the related hierarchy of such NC quantifiers. This is a much harder problem especially to determine an entanglement measure of a general two-qubit state without a full two-qubit QST. For a related discussion and references we refer to [45], where the hierarchy of entanglement, steering, and Bell nonlocality of experimental two polarization qubit states was demonstrated via a full QST. Actually such a method which enables the determination of an entanglement measure without full QST of two polarization qubits has been proposed [78], but it is quite complicated and, thus, has not been implemented experimentally yet. The determination of the Costa-Angelo steering measures $S_{CA}^{(2)}(\rho)$ and $S_{CA}^{(3)}(\rho)$ (and, thus, the corresponding Bell nonlocality and steering potentials) without full QST is possible, but the method has been so far developed only for polarization qubits [75]. To our knowledge, the only experimental work showing the hierarchy of entanglement, steering, and Bell nonlocality measures without full QST has been reported very recently in Ref. [47], but only for some specific classes of two-polarization qubits (i.e., Werner and Werner-like states). In the present paper, we study an analogous hierarchy of quantum correlations, but for single-qubit states. These states, after mixing with the vacuum on a balanced or unbalanced BS and subjected to phase damping result in two-qubit states belonging to much broader classes of states than the Werner and Werner-like states.

B. Nonclassical potentials for higher-dimensional single-mode optical states

One can apply NC potentials not only for VOPS states, but also for single-mode optical states of higher dimensions, and (at least for some classes of) continuous-variable (CV) states. We can interpret such potentials in close analogy to those for single-qubit states by applying the Wiseman *et al.* interpretation of the corresponding two-mode NC correlations [57]. Specifically, an EPR steering potential describes the quantum correlations exhibited by a single-mode bosonic field, enabling the verification of two-mode entanglement, generated by a linear coupling of the single-mode field with the vacuum, even when complete characterization of one of the generated modes is lacking. While the Bell nonlocality (entanglement) potentials describe single-mode nonclassical correlations in the case when complete characteri-

zation of both generated modes is lacking (available).

The calculation of steering and Bell nonlocality potentials based on measures of the corresponding two-mode correlations would be very challenging numerically, except low-dimensional qudits or specific classes of CV states (like Gaussian states). In particular, the calculation of steering potentials based on two-mode steering measures for two qutrits can be effectively performed by applying semidefinite programming [16]. Anyway, such a measure-based approach becomes numerically demanding already for two quartits. Thus, it is much more practical to analyze single-mode steering and nonlocality potentials for qudits and CV systems based on necessary and sufficient criteria, corresponding to violations of some classical inequalities for observing two-mode correlations, instead of analyzing their measures. Thus, the hierarchies of criteria of steering and nonlocality potentials for single-mode fields can be determined via the hierarchies of sufficient or necessary conditions for observing, respectively, two-mode steering (e.g., [22]) and nonlocality (e.g., [51]).

The calculations of steering and Bell nonlocality potentials can usually be much simplified by limiting the number of measurements from infinite to finite, as we have assumed even in our analysis of single-qubit states. A variety of powerful Bell and steering inequalities, which can be readily applied for calculating the corresponding potentials beyond the VOPS states and beyond the applied measurement scenarios, are reviewed in Refs. [18] and [16, 17], respectively. Steering witnesses for CV systems can be based on the variances of some observables [103] or entropic uncertainty relations [104, 105]. We also note that Bell inequalities, which can be the basis for defining the nonlocality potentials for CV systems, have been studied even for the infinite number of measurement settings of each party [106, 107] and for continuous sets of values of the measurement outputs [108, 109].

Such an analysis of NC potentials for CV states, can be much simplified by limiting the interest to Gaussian states, i.e., displaced squeezed thermal states. Actually, an entanglement potential based on the logarithmic negativity was applied to Gaussian states already in the first paper on NC potentials [34]. The convertibility (via a BS) of locally squeezed Gaussian states and entanglement was considered in Ref. [110]. Concerning steering potentials, one can use a computable measure of steering for arbitrary bipartite Gaussian states proposed in [111]. Nonlocality potentials for Gaussian states can be considered via Bell's inequality violations using homodyne detection, as studied in, e.g., [112].

VI. CONCLUSIONS

We have studied theoretically measures of various types of single-qubit quantum correlations related to two-qubit correlations via a linear transformation. Thus, we have generalized the concept of entanglement potentials

of Asbóth *et al.* [34], as measures of single-mode NC, by proposing the Bell nonlocality and steering potentials. Analogously to the Wiseman *et al.* standard interpretation of entanglement, steering, and Bell nonlocality of two-party systems [57], one can interpret NC correlations of single-qubit states with nonvanishing potentials via trusted or untrusted detectors used for measuring the two-qubit states, which are generated via balanced beam-splitting on the single-qubit ones.

We have applied this approach for quantifying the nonclassicality of VOPS states by mixing them with the vacuum on a balanced BS and then to determine various measures of two-qubit (two-mode) nonclassical correlations. Specifically, we have applied here: (i) the negativity and concurrence as examples of entanglement potentials; (ii) quantum steering potentials based on the Costa-Angelo measures [66] of two-qubit steering in the three-measurement scenario via the maximal violation of a CJWR inequality. We have chosen these specific steering potentials as they can be calculated analytically for any two-qubit states. We note that steering potentials can be defined and applied (at least numerically) via other popular steering measures, like the steerable weight [67] and the steering robustness [68], which also might be applied for studying steering potentials for two qudit states. Moreover, we have defined a Bell nonlocality potential via the Horodecki measure [73] of two-qubit Bell nonlocality quantifying the maximal violation of the Bell-CHSH inequality. We note that this potential is monotonically related to the steering potential based on the Costa-Angelo measure in the two-measurement scenario [66]. Thus, with the help of these potentials, we could reveal the hierarchy of single-qubit nonclassical correlations in analogy to the hierarchy of the corresponding two-qubit correlations [45, 47]. We have discussed various methods for the generation of VOPS states and the homodyne tomographic reconstruction of the resulting two-mode states and the calculation of realistic potentials assuming system imperfections including phase damping and unbalanced beam splitting.

The studied hierarchy of single-qubit potentials for generating two-qubit entanglement, steering, and Bell nonlocality can also be useful for estimating the degree of one type of quantum correlation from another, e.g., estimating the Bell nonlocality or steering potentials from an entanglement potential (or vice versa), in the spirit of such estimations for the corresponding two-qubit quantum-correlation measures (see, e.g., [113] and references therein).

Apart from a fundamental interest in single-photon entanglement and VOPS states, these have been experimentally used for quantum information tasks, including quantum teleportation [23, 88] and EPR steering [26]. Moreover, one can subject a VOPS to a non-demolition photon presence detection gate and to partially erase this information [114]. Thus, we believe that a deeper study NC correlations of VOPS states can find further applications for quantum technologies.

We also stress that the studied NC potentials are not limited to Fock-state superpositions. Indeed, the results of this paper can be experimentally implemented with qubits encoded in, e.g., photon polarization, as reported in Ref. [115]. Thus, we believe that our work can stimulate further research in quantifying and utilizing the NC of single-mode optical fields in close analogy to various types of intermode quantum correlations with applications for quantum information processing.

ACKNOWLEDGMENTS

A.M. and K.B. are supported by the Polish National Science Centre (NCN) under the Maestro Grant No. DEC-2019/34/A/ST2/00081. J.K. acknowledges Internal Palacký University grant No. IGA_PrF_2023_005. F.N. is supported in part by: Nippon Telegraph and Telephone Corporation (NTT) Research, the Japan Science and Technology Agency (JST) [via the Quantum Leap Flagship Program (Q-LEAP), and the Moonshot R&D Grant Number JPMJMS2061], the Asian Office of Aerospace Research and Development (AOARD) (via Grant No. FA2386-20-1-4069), and the Foundational Questions Institute Fund (FQXi) via Grant No. FQXi-IAF19-06.

Appendix A: Cahill-Glauber s -parametrized quasiprobability distributions

Here we recall some basic formulas of the Cahill-Glauber formalism of quasiprobability distributions (QPD) [116], which are phase-space representations of single- or multimode states. These are generalizations of the standard Wigner, Husimi, and Glauber-Sudarshan functions.

For a multimode optical state ρ , the Cahill-Glauber s -parametrized QPD is defined as

$$\mathcal{W}^{(s)}(\{\alpha_k\}) = \frac{1}{\pi^M} \langle T^{(s)}(\{\alpha_k\}) \rangle = \frac{1}{\pi^M} \text{Tr} \left[\rho \prod_k T^{(s)}(\alpha_k) \right], \quad (\text{A1})$$

where $s \in [-1, 1]$, $\{\alpha_k\} = (\alpha_1, \dots, \alpha_M)$ (for the studied states ρ_{out} , the number of modes is $M = 2$), α_k are complex numbers, and the k th-mode operator $T^{(s)}(\alpha_k)$ is defined by

$$T^{(s)}(\alpha_k) = \int D^{(s)}(\beta_k) \exp(\alpha_k \beta_k^* - \alpha_k^* \beta_k) \frac{d^2 \beta_k}{\pi}, \quad (\text{A2})$$

which is the Fourier transform of the s -parametrized displacement operator,

$$D^{(s)}(\beta_k) = \exp \left(\beta_k a_k^\dagger - \beta_k^* a_k + \frac{s}{2} |\beta_k|^2 \right), \quad (\text{A3})$$

where a_k (a_k^\dagger) is the k th-mode annihilation (creation) operator. The multimode operator $T^{(s)}(\{\alpha_k\})$ is just a

product of single-mode operators $T^{(s)}(\alpha_k)$, which can be equivalently defined as

$$T^{(s)}(\alpha_k) = \frac{2}{1-s} D(\alpha_k) \left(\frac{s+1}{1-s} \right)^{a_k^\dagger a_k} D^{-1}(\alpha_k), \quad (\text{A4})$$

where $D(\alpha_k) = D^{(0)}(\alpha_k)$ is the standard displacement operator. In the three special cases of $s = -1, 0, 1$, the s -parameterized QPD, $\mathcal{W}^{(s)}(\alpha_1, \alpha_2)$, reduces, respectively, to the Husimi Q , Wigner W , and Glauber-Sudarshan P functions corresponding to the antinormal, symmetric, and normal orderings of the creation and annihilation operators. After substituting Eq. (A4) to Eq. (A1) for $s = 0$, one arrives at

$$\begin{aligned} W(\{\alpha_k\}) &\equiv W^{(0)}(\{\alpha_k\}) \\ &= \frac{2}{\pi^M} \text{Tr} \left[\rho \prod_k D(\alpha_k) \mathcal{P}(a_k) D^{-1}(\alpha_k) \right], \end{aligned} \quad (\text{A5})$$

where $\mathcal{P}(a_k) = (-1)^{a_k^\dagger a_k}$ is the photon-number parity operator. The Cahill-Glauber formula in Eq. (A6) is the basis for a direct experimental measurement of the single-mode [90, 101] and multimode Wigner functions just by performing proper displacements $D(\alpha_k)$ in the phase space and the measurements of the parity operator $\mathcal{P}(a_k)$.

The QPD for any s contains a full information about a given state ρ , as implied by the formula

$$\rho = \int \mathcal{W}^{(s)}(\{\alpha_k\}) T^{(-s)}(\{\alpha_k\}) d^2\{\alpha_k\}, \quad (\text{A6})$$

where $d^2\{\alpha_k/\pi\} = d^2\alpha_1 \cdots d^2\alpha_M$. For numerical calculations of a QPD (practically for any s , which is not too close to 1), it is useful to use its Fock-state representa-

tion,

$$\begin{aligned} \mathcal{W}^{(s)}(\{\alpha_k\}) &= \frac{1}{\pi^M} \sum_{\{m_k\}=0}^{N_0} \sum_{\{n_k\}=0}^{N_0} \prod_{k=1}^M \langle n_k | T^{(s)}(\alpha_k) | m_k \rangle, \\ &\times \langle \{n_k\} | \rho | \{m_k\} \rangle, \end{aligned} \quad (\text{A7})$$

where

$$\begin{aligned} \langle n_k | T^{(s)}(\alpha_k) | m_k \rangle &= \sqrt{\frac{n_k!}{m_k!}} \left(\frac{-s_m}{s_p} \right)^{n_k} s_m^{\delta_k+1} (\alpha_k^*)^{\delta_k} \\ &\times L_{n_k}^{(\delta_k)}(s_p s_m |\alpha_k|^2) \exp(-s_m |\alpha_k|^2), \end{aligned} \quad (\text{A8})$$

for $m_k \geq n_k$; other elements can be found from the property $\langle n_k | T^{(s)}(\alpha_k) | m_k \rangle = \langle m_k | T^{(s)}(\alpha_k^*) | n_k \rangle$. Here $\delta_k = m_k - n_k$, $s_p = 2/(1+s)$, $s_m = 2/(1-s)$, and $L_{n_k}^{(\delta_k)}(x)$ are the associated Laguerre polynomials. To calculate the QPD for a given $s < 1$, we can directly apply the density matrices given in Eqs. (3) and (30) to Eq. (A8). The formula in Eq. (A8) can be applied even in the limit $s \rightarrow 1$, but the limit should be taken very carefully.

We note that for the VOPS states σ and the BS-transformed states ρ_{out} , it is enough to analyze the two special cases of the polynomials: $L_0^{(\delta_k)}(x) = 1$ and $L_1^{(\delta_k)}(x) = 1 + \delta_k - x$, because $N_0 = 1$. Thus, by denoting $T_{nm}^{(s)}(\alpha) = \langle n | T^{(s)}(\alpha) | m \rangle$, we have

$$\begin{aligned} T_{00}^{(s)}(\alpha) &= \frac{2}{1-s} \exp\left(-\frac{2}{1-s} |\alpha|^2\right), \\ T_{10}^{(s)}(\alpha) &= [T_{01}^{(s)}(\alpha)]^* = \frac{4\alpha}{(1-s)^2} \exp\left(-\frac{2}{1-s} |\alpha|^2\right), \\ T_{11}^{(s)}(\alpha) &= \frac{2(4|\alpha|^2 + s^2 - 1)}{(1-s)^3} \exp\left(-\frac{2}{1-s} |\alpha|^2\right). \end{aligned} \quad (\text{A9})$$

-
- [1] E. H. Kennard, Zur Quantenmechanik einfacher Bewegungstypen, *Z. Phys.* **44**, 326 (1927).
 - [2] H. J. Kimble, M. Dagenais, and L. Mandel, Photon antibunching in resonance fluorescence, *Phys. Rev. Lett.* **39**, 691 (1977).
 - [3] J. Abadie *et al.* (LIGO Scientific Collaboration), A gravitational wave observatory operating beyond the quantum shot-noise limit, *Nat. Phys.* **7**, 962 (2011).
 - [4] J. Aasi *et al.*, Enhanced sensitivity of the LIGO gravitational wave detector by using squeezed states of light, *Nat. Photonics* **7**, 613 (2013).
 - [5] H. Grote, K. Danzmann, K. L. Dooley, R. Schnabel, J. Slutsky, and H. Vahlbruch, First Long-Term Application of Squeezed States of Light in a Gravitational-Wave Observatory, *Phys. Rev. Lett.* **110**, 181101 (2013).
 - [6] H.-S. Zhong *et al.*, Quantum computational advantage using photons, *Science* **370**, 1460 (2020).
 - [7] H.-S. Zhong *et al.*, Phase-Programmable Gaussian Boson Sampling Using Stimulated Squeezed Light, *Phys. Rev. Lett.* **127**, 180502 (2021).
 - [8] L. S. Madsen *et al.*, Quantum computational advantage with a programmable photonic processor, *Nature (London)* **606**, 75 (2022).
 - [9] J. Yin *et al.*, Entanglement-based secure quantum cryptography over 1,120 kilometres, *Nature (London)* **582**, 501 (2020).
 - [10] R. J. Glauber, *Quantum Theory of Optical Coherence: Selected Papers and Lectures* (Wiley-VCH, Weinheim, 2007).
 - [11] E. C. G. Sudarshan, Equivalence of Semiclassical and Quantum Mechanical Descriptions of Statistical Light Beams, *Phys. Rev. Lett.* **10**, 277 (1963).
 - [12] M. O. Scully and M. S. Zubairy, *Quantum Optics* (Cambridge University Press, Cambridge, UK, 1997).
 - [13] G. Agarwal, *Quantum Optics* (Cambridge University Press, Cambridge, UK, 2013).
 - [14] W. Vogel and D. G. Welsch, *Quantum Optics* (Wiley-VCH, Weinheim, 2006).
 - [15] R. Horodecki, P. Horodecki, M. Horodecki, and K. Horodecki, Quantum entanglement, *Rev. Mod. Phys.*

- 81**, 865 (2009).
- [16] D. Cavalcanti and P. Skrzypczyk, Quantum steering: a review with focus on semidefinite programming, *Rep. Prog. Phys.* **80**, 024001 (2017).
- [17] R. Uola, A. C. S. Costa, H. C. Nguyen, and O. Gühne, Quantum steering, *Rev. Mod. Phys.* **92**, 015001 (2020).
- [18] N. Brunner, D. Cavalcanti, S. Pironio, V. Scarani, and S. Wehner, Bell nonlocality, *Rev. Mod. Phys.* **86**, 419 (2014).
- [19] S. M. Tan, D. F. Walls, and M. J. Collett, Nonlocality of a Single Photon, *Phys. Rev. Lett.* **66**, 252 (1991).
- [20] L. Hardy, Nonlocality of a Single Photon Revisited, *Phys. Rev. Lett.* **73**, 2279 (1994).
- [21] S. J. Jones and H. M. Wiseman, Nonlocality of a single photon: Paths to an Einstein-Podolsky-Rosen-steering experiment, *Phys. Rev. A* **84**, 012110 (2011).
- [22] I. Kogias, P. Skrzypczyk, D. Cavalcanti, A. Acin, and G. Adesso, Hierarchy of Steering Criteria Based on Moments for All Bipartite Quantum Systems, *Phys. Rev. Lett.* **115**, 210401 (2015).
- [23] E. Lombardi, F. Sciarrino, S. Popescu, and F. De Martini, Teleportation of a Vacuum-One-Photon Qubit, *Phys. Rev. Lett.* **88**, 070402 (2002).
- [24] A. I. Lvovsky and J. H. Shapiro, Nonclassical character of statistical mixtures of the single-photon and vacuum optical states, *Phys. Rev. A* **65**, 033830 (2002).
- [25] S. A. Babichev, J. Appel, and A. I. Lvovsky, Homodyne Tomography Characterization and Nonlocality of a Dual-Mode Optical Qubit, *Phys. Rev. Lett.* **92**, 193601 (2004).
- [26] M. Fuwa, S. Takeda, M. Zwierz, H.M. Wiseman, and A. Furusawa, Experimental proof of nonlocal wavefunction collapse for a single particle using homodyne measurements, *Nat. Commun.* **6**, 6665 (2015).
- [27] V. V. Dodonov and V. I. Man'ko (eds.), *Theory of Nonclassical States of Light* (Taylor & Francis, New York, 2003).
- [28] J. Peřina, Z. Hradil, and B. Jurčo, *Quantum Optics and Fundamentals of Physics* (Kluwer, Dordrecht, 1994).
- [29] A. Miranowicz, M. Bartkowiak, X. Wang, Y. X. Liu, and F. Nori, Testing nonclassicality in multimode fields: a unified derivation of classical inequalities, *Phys. Rev. A* **82**, 013824 (2010).
- [30] M. Bartkowiak, A. Miranowicz, X. Wang, Y.X. Liu, W. Leoński, and F. Nori, Sudden vanishing and reappearance of nonclassical effects: General occurrence of finite-time decays and periodic vanishings of nonclassicality and entanglement witnesses, *Phys. Rev. A* **83**, 053814 (2011).
- [31] M. Hillery, Nonclassical distance in quantum optics, *Phys. Rev. A* **35**, 725 (1987).
- [32] C. T. Lee, Measure of the nonclassicality of nonclassical states, *Phys. Rev. A* **44**, R2775 (1991).
- [33] N. Lütkenhaus and S. M. Barnett, Nonclassical effects in phase space, *Phys. Rev. A* **51**, 3340 (1995).
- [34] J. K. Asbóth, J. Calsamiglia, and H. Ritsch, Computable measure of nonclassicality for light, *Phys. Rev. Lett.* **94**, 173602 (2005).
- [35] A. Miranowicz, K. Bartkiewicz, A. Pathak, J. Peřina Jr., Y. N. Chen, and F. Nori, Statistical mixtures of states can be more quantum than their superpositions: Comparison of nonclassicality measures for single-qubit states, *Phys. Rev. A* **91**, 042309 (2015).
- [36] I. I. Arkhipov, J. Peřina Jr., J. Peřina, and A. Miranowicz, Comparative study of nonclassicality, entanglement, and dimensionality of multimode noisy twin beams, *Phys. Rev. A* **91**, 033837 (2015).
- [37] A. Kenfack and K. Życzkowski, Negativity of the Wigner function as an indicator of non-classicality, *J. Opt. B* **6**, 396 (2004).
- [38] A. Mari, K. Kieling, B. M. Nielsen, E. S. Polzik, and J. Eisert, Directly Estimating Nonclassicality, *Phys. Rev. Lett.* **106**, 010403 (2011).
- [39] W. Vogel and J. Sperling, Unified quantification of nonclassicality and entanglement, *Phys. Rev. A* **89**, 052302 (2014).
- [40] A. Miranowicz, K. Bartkiewicz, N. Lambert, Y.-N. Chen, F. Nori, Increasing relative nonclassicality quantified by standard entanglement potentials by dissipation and unbalanced beam splitting, *Phys. Rev. A* **92**, 062314 (2015).
- [41] N. Killoran, F. E. S. Steinhoff, and M. B. Plenio, Converting non-classicality into entanglement, *Phys. Rev. Lett.* **116**, 080402 (2016).
- [42] C. Gehrke, J. Sperling, and W. Vogel, Quantification of nonclassicality, *Phys. Rev. A* **86**, 052118 (2012).
- [43] S. Meznaric, S. R. Clark, and A. Datta, Quantifying the Nonclassicality of Operations, *Phys. Rev. Lett.* **110**, 070502 (2013).
- [44] T. Nakano, M. Piani, and G. Adesso, Negativity of quantumness and its interpretations, *Phys. Rev. A* **88**, 012117 (2013).
- [45] K. Jiráková, A. Černocho, K. Lemr, K. Bartkiewicz, and A. Miranowicz, Experimental hierarchy and optimal robustness of quantum correlations of two-qubit states with controllable white noise, *Phys. Rev. A* **104**, 062436 (2021).
- [46] H.-Y. Ku, J. Kadlec, A. Černocho, M. T. Quintino, W. Zhou, K. Lemr, N. Lambert, A. Miranowicz, S.-L. Chen, F. Nori, and Y.-N. Chen, Quantifying Quantumness of Channels Without Entanglement, *PRX Quantum* **3**, 020338 (2022).
- [47] S. Abo, J. Soubusta, K. Jiráková, K. Bartkiewicz, A. Černocho, K. Lemr, A. Miranowicz, Experimental hierarchy of two-qubit quantum correlations without state tomography, *Sci. Rep.* **13**, 8564 (2023).
- [48] H.Y. Ku, S.L. Chen, N. Lambert, Y.N. Chen, and F. Nori, Hierarchy in temporal quantum correlations, *Phys. Rev. A* **98**, 022104 (2018).
- [49] E. Shchukin and W. Vogel, Inseparability Criteria for Continuous Bipartite Quantum States, *Phys. Rev. Lett.* **95**, 230502 (2005).
- [50] A. Miranowicz and M. Piani, Comment on Inseparability Criteria for Continuous Bipartite Quantum States, *Phys. Rev. Lett.* **97**, 058901 (2006).
- [51] M. Navascués, S. Pironio, and A. Acín, Bounding the Set of Quantum Correlations, *Phys. Rev. Lett.* **98**, 010401 (2007).
- [52] T. Richter and W. Vogel, Nonclassicality of Quantum States: A Hierarchy of Observable Conditions, *Phys. Rev. Lett.* **89**, 283601 (2002).
- [53] W. Vogel, Nonclassical Correlation Properties of Radiation Fields, *Phys. Rev. Lett.* **100**, 013605 (2008).
- [54] A. Miranowicz, K. Bartkiewicz, J. Peřina Jr., M. Koashi, N. Imoto, and F. Nori, Optimal two-qubit tomography based on local and global measurements: Maximal robustness against errors as described by condition numbers, *Phys. Rev. A* **90**, 062123 (2014).

- [55] K. Bartkiewicz, A. Černoč, K. Lemr, A. Miranowicz, Priority Choice Experimental Two-qubit Tomography: Measuring One by One All Elements of Density Matrices, *Sci. Rep.* **6**, 19610 (2016),
- [56] W. K. Wootters, Entanglement of Formation of an Arbitrary State of Two Qubits, *Phys. Rev. Lett.* **80**, 2245 (1998).
- [57] H. M. Wiseman, S. J. Jones, and A. C. Doherty, Steering, Entanglement, Nonlocality, and the Einstein-Podolsky-Rosen Paradox, *Phys. Rev. Lett.* **98**, 140402 (2007).
- [58] B. Yadin, M. Fadel, and M. Gessner, Metrological complementarity reveals the Einstein-Podolsky-Rosen paradox, *Nat. Commun.* **12**, 2410 (2021).
- [59] K.Y. Lee, J.D. Lin, A. Miranowicz, F. Nori, H.Y. Ku, and Y.N. Chen, Steering-enhanced quantum metrology using superpositions of noisy phase shifts, *Phys. Rev. Research* **5**, 013103 (2023).
- [60] Y.N. Chen, C.M. Li, N. Lambert, S.L. Chen, Y. Ota, G.Y. Chen, and F. Nori, Temporal steering inequality *Phys. Rev. A* **89**, 032112 (2014).
- [61] K. Bartkiewicz, A. Černoč, K. Lemr, A. Miranowicz, and F. Nori, Experimental temporal quantum steering, *Sci. Rep.* **6**, 38076 (2016).
- [62] S.L. Chen, N. Lambert, C.M. Li, G.Y. Chen, Y.N. Chen, A. Miranowicz, and F. Nori, Spatio-Temporal Steering for Testing Nonclassical Correlations in Quantum Networks, *Sci. Rep.* **7**, 3728 (2017).
- [63] K. Bartkiewicz, A. Černoč, K. Lemr, A. Miranowicz, and F. Nori, Temporal steering and security of quantum key distribution with mutually unbiased bases against individual attacks *Phys. Rev. A* **93**, 062345 (2016).
- [64] S.L. Chen, N. Lambert, C.M. Li, A. Miranowicz, Y.N. Chen, and F. Nori, Quantifying Non-Markovianity with Temporal Steering *Phys. Rev. Lett.* **116**, 020503 (2016).
- [65] J.D. Lin, W.Y. Lin, H.Y. Ku, N. Lambert, Y.N. Chen, F. Nori Quantum steering as a witness of quantum scrambling, *Phys. Rev. A* **104**, 022614 (2021).
- [66] A. C. S. Costa and R. M. Angelo, Quantification of Einstein-Podolski-Rosen steering for two-qubit states, *Phys. Rev. A* **93**, 020103 (2016).
- [67] P. Skrzypczyk, M. Navascués, and D. Cavalcanti, Quantifying Einstein-Podolsky-Rosen Steering, *Phys. Rev. Lett.* **112**, 180404 (2014).
- [68] M. Piani and J. Watrous, Necessary and Sufficient Quantum Information Characterization of Einstein-Podolsky-Rosen Steering, *Phys. Rev. Lett.* **114**, 060404 (2015).
- [69] X.-G. Fan, H. Yang, F. Ming, D. Wang, and L. Ye, Constraint Relation Between Steerability and Concurrence for Two-Qubit States, *Ann. der Physik* **533**, 2100098 (2021).
- [70] H. Yang, F. Zhao, X.-G. Fan, Z.-Y. Ding, D. Wang, X.-K. Song, H. Yuan, C.-J. Zhang, and L. Ye, Estimating quantum steering and Bell nonlocality through quantum entanglement in two-photon systems, *Opt. Express* **29**, 26822 (2021).
- [71] E. G. Cavalcanti, S. J. Jones, H. M. Wiseman, and M. D. Reid, Experimental criteria for steering and the Einstein-Podolsky-Rosen paradox, *Phys. Rev. A* **80**, 032112 (2009).
- [72] J. F. Clauser, M. A. Horne, A. Shimony, and R. A. Holt, Proposed Experiment to Test Local Hidden-Variable Theories, *Phys. Rev. Lett.* **23**, 880 (1969).
- [73] R. Horodecki, P. Horodecki, and M. Horodecki, Violating Bell inequality by mixed states: necessary and sufficient condition, *Phys. Lett. A* **200**, 340 (1995).
- [74] A. Miranowicz, Violation of Bell inequality and entanglement of decaying Werner states, *Phys. Lett. A* **327**, 272 (2004).
- [75] K. Bartkiewicz, K. Lemr, A. Černoč, and A. Miranowicz, Bell nonlocality and fully entangled fraction measured in an entanglement-swapping device without quantum state tomography, *Phys. Rev. A* **95**, 030102 (2017).
- [76] M. A. Nielsen and I. L. Chuang, *Quantum Computation and Quantum Information* (Cambridge University Press, Cambridge, 2000).
- [77] R. Augusiak, M. Demianowicz, and P. Horodecki, Universal observable detecting all two-qubit entanglement and determinant-based separability tests, *Phys. Rev. A* **77**, 030301 (2008).
- [78] K. Bartkiewicz, P. Horodecki, K. Lemr, A. Miranowicz, and K. Życzkowski, Method for universal detection of two-photon polarization entanglement, *Phys. Rev. A* **91**, 032315 (2015).
- [79] U. Leonhardt, *Measuring the Quantum State of Light* (Cambridge University Press, Cambridge, 1997).
- [80] C. Eichler, D. Bozyigit, C. Lang, M. Baur, L. Steffen, J. M. Fink, S. Filipp, and A. Wallraff, Observation of Two-Mode Squeezing in the Microwave Frequency Domain, *Phys. Rev. Lett.* **107**, 113601 (2011).
- [81] S. M. Rochester and D. Budker, Atomic polarization visualized, *Am. J. Phys.* **69**(4), 450 (2001).
- [82] E. B. Alexandrov, M. Auzinsh, D. Budker, D. F. Kimball, S. M. Rochester, and V. V. Yashchuk, Dynamic effects in nonlinear magneto-optics of atoms and molecules: review, *J. Opt. Soc. Am. B* **22**, 7 (2005).
- [83] M. Auzinsh, D. Budker, and S. M. Rochester, *Optically Polarized Atoms: Understanding Light-Atom Interactions* (Oxford University press, Oxford, 2014).
- [84] G. S. Agarwal, Relation between atomic coherent-state representation, state multipoles, and generalized phase-space distributions, *Phys. Rev. A* **24**, 2889 (1981).
- [85] J. P. Dowling, G. S. Agarwal, and W. P. Schleich, Wigner distribution of a general angular-momentum state: Applications to a collection of two-level atoms, *Phys. Rev. A* **49**, 4101 (1994).
- [86] K. J. Resch, J. S. Lundeen, and A. M. Steinberg, Quantum State Preparation and Conditional Coherence, *Phys. Rev. Lett.* **88**, 113601 (2002).
- [87] A. I. Lvovsky and J. Mlynek, Quantum-Optical Catalysis: Generating Nonclassical States of Light by Means of Linear Optics, *Phys. Rev. Lett.* **88**, 250401 (2002).
- [88] S. A. Babichev, J. Ries, and A. I. Lvovsky, Quantum scissors: teleportation of single-mode optical states by means of a nonlocal single photon, *Europhys. Lett.* **64**, 1 (2003).
- [89] V. Magro, J. Vaneecloo, S. Garcia, and A. Ourjoumtsev, Deterministic freely propagating photonic qubits with negative Wigner functions, *Nat. Photon.* (2023) <https://doi.org/10.1038/s41566-023-01196-y>
- [90] M. Hofheinz *et al.*, Synthesizing arbitrary quantum states in a superconducting resonator, *Nature (London)* **459**, 546 (2009).
- [91] S. M. Barnett and D. T. Pegg, Phase Measurement by Projection Synthesis, *Phys. Rev. Lett.* **76**, 4148 (1996).
- [92] S. K. Özdemir, A. Miranowicz, M. Koashi, and N.

- Imoto, Quantum-scissors device for optical state truncation: A proposal for practical realization, *Phys. Rev. A* **64**, 063818 (2001).
- [93] S. K. Özdemir, A. Miranowicz, M. Koashi, and N. Imoto: Pulse-mode quantum projection synthesis: Effects of mode mismatch on optical state truncation and preparation, *Phys. Rev. A* **66**, 053809 (2002).
- [94] T. C. Ralph and A. P. Lund, Nondeterministic Noiseless Linear Amplification of Quantum Systems, *AIP Conf. Proc.* **1110**, 155 (2009).
- [95] S. Deleglise *et al.*, Reconstruction of non-classical cavity field states with snapshots of their decoherence, *Nature (London)* **455**, 510 (2008).
- [96] A. A. Houck *et al.*, Generating single microwave photons in a circuit, *Nature (London)* **449**, 328 (2007).
- [97] M. A. Sillanpää, J. I. Park, and R. W. Simmonds, Coherent quantum state storage and transfer between two phase qubits via a resonant cavity, *Nature (London)* **449**, 438 (2007).
- [98] A. D. Boozer *et al.*, Reversible state transfer between light and a single trapped atom, *Phys. Rev. Lett.* **98**, 193601 (2007).
- [99] A. Ben-Kish *et al.*, Experimental demonstration of a technique to generate arbitrary quantum superposition states of a harmonically bound spin-1/2 particle, *Phys. Rev. Lett.* **90**, 037902 (2003).
- [100] G. M. D'Ariano, L. Maccone, M. F. Sacchi, A. Garuccio, Tomographic test of Bell's inequality, *J. Opt. B* **1**, 576 (1999).
- [101] L. G. Lutterbach and L. Davidovich, Method for Direct Measurement of the Wigner Function in Cavity QED and Ion Traps, *Phys. Rev. Lett.* **78**, 2547 (1997).
- [102] Ch. Wang *et al.*, A Schrödinger cat living in two boxes, *Science* **352**, 1087 (2016).
- [103] M. D. Reid, Demonstration of the Einstein-Podolsky-Rosen paradox using nondegenerate parametric amplification, *Phys. Rev. A* **40**, 913 (1989).
- [104] S. P. Walborn, A. Salles, R. M. Gomes, F. Toscano, and P. H. Souto Ribeiro, Revealing Hidden Einstein-Podolsky-Rosen Nonlocality, *Phys. Rev. Lett.* **106**, 130402 (2011).
- [105] J. Schneeloch, P. B. Dixon, G. A. Howland, C. J. Broadbent, and J. C. Howell, Violation of Continuous-Variable Einstein-Podolsky-Rosen Steering with Discrete Measurements, *Phys. Rev. Lett.* **110**, 130407 (2013).
- [106] D. Kaszlikowski and M. Zukowski, Bell theorem involving all possible local measurements, *Phys. Rev. A* **61**, 022114 (1999).
- [107] N. Aharon, S. Machnes, B. Reznik, J. Silman, and L. Vaidman, 2012, Continuous input nonlocal games, *Natural Comp.* **12**, 5 (2013).
- [108] E. G. Cavalcanti, C. J. Foster, M. D. Reid, and P. D. Drummond, Bell Inequalities for Continuous-Variable Correlations, *Phys. Rev. Lett.* **99**, 210405 (2007).
- [109] A. Salles, D. Cavalcanti, A. Acín, D. Pérez-García, and M. M. Wolf, Bell inequalities from multilinear contractions, *Quant. Inf. Comp.* **10**, 703 (2010).
- [110] I.I. Arkhipov, J. Peřina Jr., J. Svozilík, A. Miranowicz, Nonclassicality Invariant of Bipartite Gaussian States, *Sci. Rep.* **6**, 26523 (2016).
- [111] I. Kogias, A. R. Lee, S. Ragy, and G. Adesso, Quantification of Gaussian Quantum Steering, *Phys. Rev. Lett.* **114**, 060403 (2015).
- [112] M. Paternostro, H. Jeong, and T. C. Ralph, Violations of Bell's inequality for Gaussian states with homodyne detection and nonlinear interactions, *Phys. Rev. A* **79**, 012101 (2009).
- [113] K. Bartkiewicz, B. Horst, K. Lemr, and A. Miranowicz, Entanglement estimation from Bell inequality violation, *Phys. Rev. A* **88**, 052105 (2013).
- [114] J. Roik, K. Lemr, A. Černoč, and K. Bartkiewicz, Interplay between strong and weak measurement: comparison of three experimental approaches to weak value estimation, *J. Opt.* **22**, 065202 (2020).
- [115] J. Kadlec, K. Bartkiewicz, A. Černoč, K. Lemr, and A. Miranowicz, Experimental hierarchy of the nonclassicality of single-qubit states via potentials for entanglement, steering, and Bell nonlocality, e-print arXiv:2308.xxx (2023).
- [116] K. E. Cahill and R. J. Glauber, Ordered Expansions in Boson Amplitude Operators, *Phys. Rev.* **177**, 1857 (1969); Density Operators and Quasiprobability Distributions, *ibid.*, 1882 (1969).